Chemical Speciation of PM$_{10}$ at Swiss Cottage

October 2009

David Green, Anja Tremper and Gary Fuller

Environmental Research Group

King's College London

Title	Chemical Speciation of PM_{10} at Swiss Cottage

Customer	London Borough of Camden
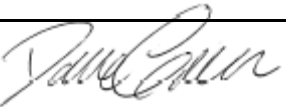
Customer Ref	-
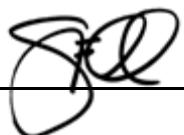
File Reference	ERG\Airquali\LA\Camden\ChemicalCharacterisation\SwissCottagePM10.doc
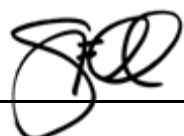
Environmental Research Group
King's College London
4th Floor
Franklin-Wilkins Building
150 Stamford St
London SE1 9NH
Tel 020 7848 4044
Fax 020 7848 4045

	Name	Signature	Date
Authors	David Green, Anja Tremper and Gary Fuller		October 2009
Reviewed by	Gary Fuller		October 2009
Approved by	Gary Fuller		October 2009

Table of Contents

1. Summary

This study used a single sampler at the London Borough of Camden's Swiss Cottage monitoring site collect PM$_{10}$ onto filters; these filters were then analysed for a range of chemical components. The results of these analyses were combined with measurements made at other sites in London to provide an assessment of the chemical composition at this site on a daily basis. This could then be compared to the independently measured PM$_{10}$ mass to examine whether the all the mass was accounted for; this is called mass closure.

The results showed that approximately two thirds of PM$_{10}$ can be considered secondary or natural, being made up of PM formed from gaseous precursors (nitrates, sulphates and SOAM) or sea salt (chlorides). The remaining third is comprised of direct vehicle exhaust (EC and POAM), tyre and brake wear (iron oxide, POAM, metals) and minerals from windblown soil and vehicular resuspension.

This analysis provided valuable information for the understanding of emissions, the targeting of abatement strategies and the assessment of the toxicological components of PM$_{10}$. The calculation of uncertainties in the analysis will help to inform the planning and execution of future studies.

2. Introduction

This study aims to measure key chemical components of PM$_{10}$ at Swiss Cottage and use these and other measurements to divide the mass of PM$_{10}$ into its chemical composition.

PM$_{10}$ has a diverse chemical composition, it contains sulphates, nitrates, ammonium, organic material, crustal species, sea salt, hydrogen ions and water. An understanding of the contributions of these components to the mass concentration and how it is measured by different instruments is important. The chemical composition of particulate matter (PM) is not uniform. Daily variation occurs due to changes in meteorological conditions (temperature, relative humidity, wind speed, wind direction), local emissions and long range transport of PM. Seasonal variations occur due to longer term changes in these parameters. For instance, a greater portion of the semi-volatile PM will be found in the gas phase due to higher temperatures during the summer months. Spatial variations occur as a result of the proximity to sources of PM. For example, vehicle emissions will have a greater impact at traffic sites, the contribution of sea salt is greatest in coastal regions and the influence of long range transport on the concentrations of secondary PM in the UK are highest in the south and east.

Mass closure models can be used to assess the chemical make-up of PM by measuring a subset components and estimating the remaining mass through a set of assumptions. This was done in the UK by Harrison et al. (2003), across 6 European cities by Sillanpää et al. (2006), in the US by Frank (2006) and more recently on a semi-continuous basis in the US by Grover et al. (2008). Harrison et al. (2004) calculated the composition of the different fractions of PM at background and traffic locations; which included several sites in London. Figure 1 shows these results as an example of the typical contribution of the different components to PM$_{10}$; a similar approach is taken in this study.
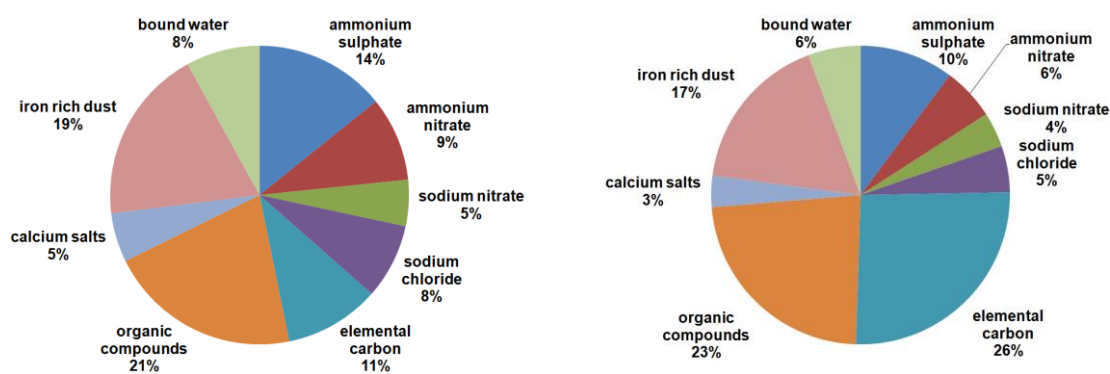
Figure 1: Composition of urban background (left) and traffic (right) PM$_{10}$. Source: (Harrison et al., 2004)

3. Method

PM$_{10}$ samples were taken at the kerbside monitoring site at Swiss Cottage between 28th October 2008 and 27th December 2008 using a Partisol 2025; the study period is defined by the availability of these samples. Measurements were also used from the background site at North Kensington and the kerbside site at Marylebone Road. The site locations and the cabins are shown in Figure 2.
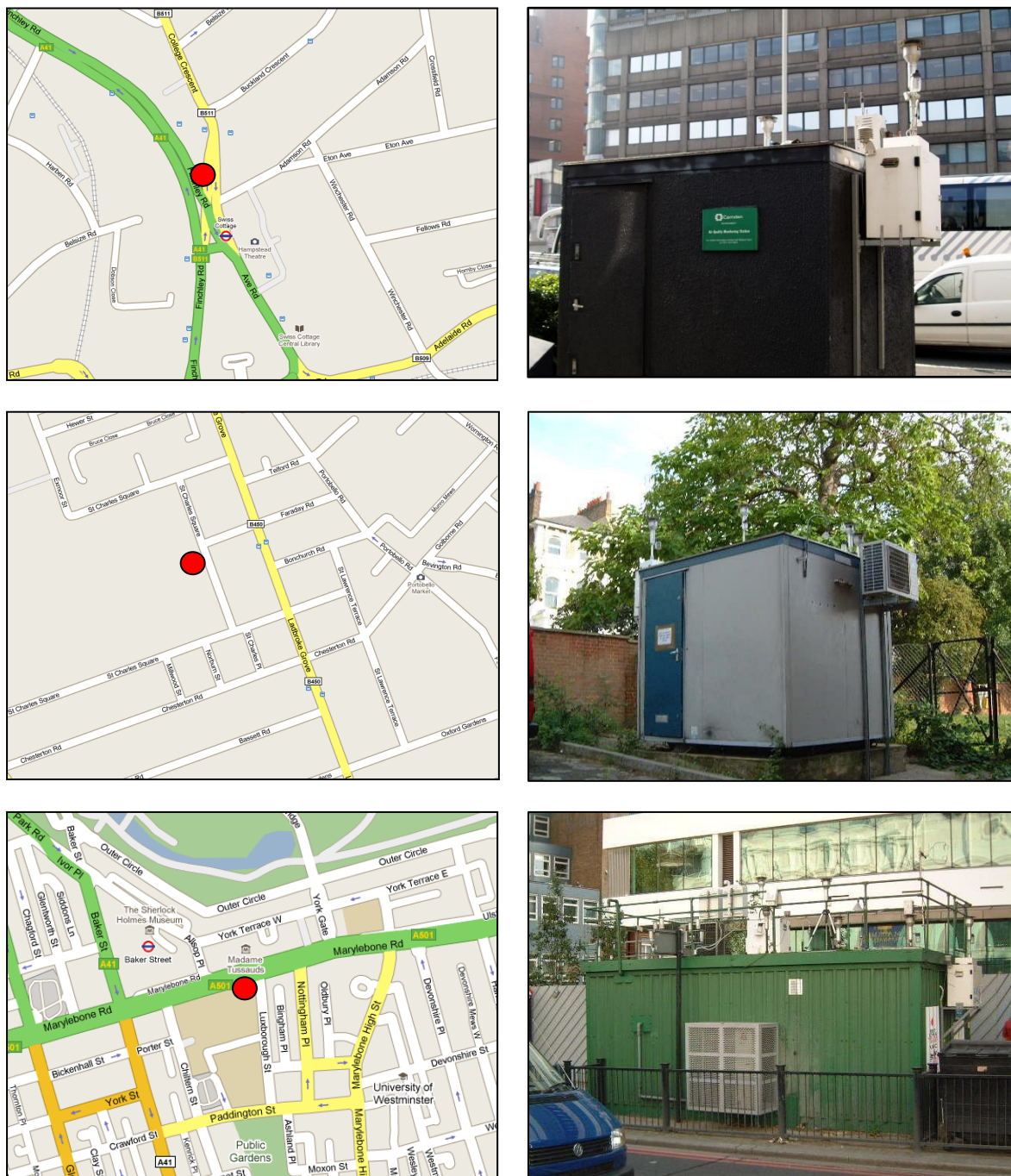
Figure 2: Monitoring sites at Swiss Cottage (top), North Kensington (middle) and Marylebone Road (bottom)

Note: Monitoring sites are marked with a red dot.

3.1. Sampling and analysis

The mass closure method used in this study utilised the measurements from real time monitoring techniques as well as chemical analysis undertaken on the sample filters collected.

3.1.1. TEOM and Volatile Correction Model (VCM)

The PM$_{10}$ mass measurement was made using a TEOM 1400AB. There is an accepted loss of semi-volatile PM from the sample due to the TEOM operating temperature of 50 ⁰C compared to the ambient sampling regime used by the gravimetric sampler (Patashnick et al., 1991; Allen et al., 1997; Smith et al., 1997). Recent work has led to the development of the Volatile Correction Model (VCM) (Green et al., 2009), which is the Defra-recommended to correct for the loss this semi-volatile fraction (Defra, 2009) from the TEOM. The PM$_{10}$ mass measurements here are reported as VCM corrected TEOM measurements and denoted TEOM$_{VCM}$.

3.1.2. Thermo 8100 Aethalometer

The Thermo 8100 aethalometer measured the carbon content of PM collected on a quartz filter paper by measurement of the light attenuation when light was passed through the filter and sample at 880 nm. It was connected to the PM$_{10}$ TEOM on the auxiliary flow line and directs 2 l min^{-1} from this flow; it therefore sampled PM$_{10}$. Analysis was continuous and the concentration was logged by the TEOM control unit and averaged to a 15 minute mean concentration. Measurements using this method demonstrated a good consistency with the Sunset elemental carbon measurements (described in section 3.1.3.2) in a previous study in London (Green et al., 2007).

3.1.3. Daily filter samples

Twenty-four hour PM$_{10}$ samples were made using a Partisol 2025; this collected PM$_{10}$ onto filters which alternated between two types of filter media (one made of quartz fibre, the other of mixed cellulose esters). Quartz fibre filters were analysed for elemental carbon (EC) and organic carbon (OC), mixed cellulose ester filters were analysed for metals. This method was chosen as only one sampler was available and no single filter media was suitable for all types of chemical analysis.

Samples from Swiss Cottage were used to calculate the concentrations of the primary pollutants such as elemental carbon. Secondary pollutants, such as ammonium nitrate and secondary organic aerosol, were assumed to be uniform over London and measurements were therefore taken from the mean of the measurements at North Kensington and Marylebone Road when they were not available from Swiss Cottage.

3.1.3.1. Sample methodology

The Thermo Partisol 2025 was designated as a US EPA reference method for PM$_{10}$ and PM$_{2.5}$ (EPA, 2004), equivalent to the EU PM$_{10}$ reference method using the requirements in EU PM$_{10}$ standard (Mückler, 1999) and to the EU reference method in the UK (Harrison, 2006). The instrument was operated at default settings and in accordance with the Defra operation manual (Maggs, 1999). The sampler incorporated a filter magazine holding 16 filter cassettes, as well as a magazine for storage allowing unattended operation for fifteen days. The filter compartment was ventilated with ambient air to maintain it within ±5 ⁰C of ambient temperature.

3.1.3.2. Sunset carbon analysis

The carbon content of PM is nominally made up of EC and OC; the concentrations of these were measured using a Sunset Laboratory carbon aerosol analysis laboratory instrument at Sunset Laboratory Inc. This is a thermal evolution method, the carbon fractions were defined by the temperatures at which they evolved in conjunction with optical correction for the conversion of OC to EC by charring. Methods such as this are subject to uncertainties due to the adsorption of carbonaceous gases onto the filter before and during sampling as well as the loss of semi-volatile organic carbon (Turpin et al., 2000), these sampling artefacts are influenced by the air flow, face velocity and filter type (Viana et al., 2006). As only one type of sampler was used in this study, the air

flow and face velocity were standardised, pre sampling positive artefacts were minimised by using heat-treated quartz fibre filters.

3.1.3.3. Ion chromatography (IC)

IC is routinely used to measure the concentration of water soluble anions in air quality networks worldwide (EMEP, 2002; EPA, 2003a; EPA, 2003b). The method used here is based on that employed by Zhou (1997) and later by Stribley (2003) from a method developed by Koutrakis et al. (1992). This method has been used in the Defra Particle Concentration and Numbers Network since 2005 (Yardley et al., 2006; Yardley et al., 2007a; Hayman et al., 2008).

3.1.3.4. Inductively coupled plasma mass spectroscopy (ICP-MS)

Concentrations of aluminium, barium, calcium, copper, iron, molybdenum, manganese, sodium, nickel, lead, antimony, strontium, vanadium and zinc in solution were determined using inductively coupled plasma mass spectrometry (ICP-MS). A 5 mm punch was taken from each filter and digested in hot acid before dilution and analysis. For a number of filters, five replicate punches were used to establish repeatability of the process.

4. Measurement results and discussion

This section sets the campaign period in the context of measurements made at Swiss Cottage during the last quarter of 2008, the winter of 2008/9 and the whole of 2008. It also presents the measurements which were used in section 5 for the mass closure analysis.

4.1.1. Representativeness of campaign

Campaign measurements are by their nature a snapshot of the pollution concentrations at the site studied, however, it is necessary to consider how representative the campaign was of these pollution concentrations. This was assessed using summary statistics of the TEOM$_{VCM}$ concentrations measured at Swiss cottage during:

1. The campaign period (28th October 2008 – 28th December 2008)
2. The quarter (1st October 2008 – 31st December 2008)
3. Winter 08/09 (1st October 2008 – 31st March 2009)
4. The year (1st January 2008 – 31st December 2008)

Figure 3 shows the mean, median, minimum, maximum, 2nd and 98th percentiles and 1st and 3rd quartiles of the PM$_{10}$ measurements. Only the 98th percentile and the maximum differ substantially between the periods analysed. This reflects the episodic nature of elevated PM$_{10}$ concentrations and the larger number of days samples in the winter and 2008 datasets. Measurements made during the campaign can therefore be considered representative of winter conditions but probably did not reflect summer periods or long range transport episodes (when concentrations of secondary PM will increase). Further campaigns would be required to examine these periods.

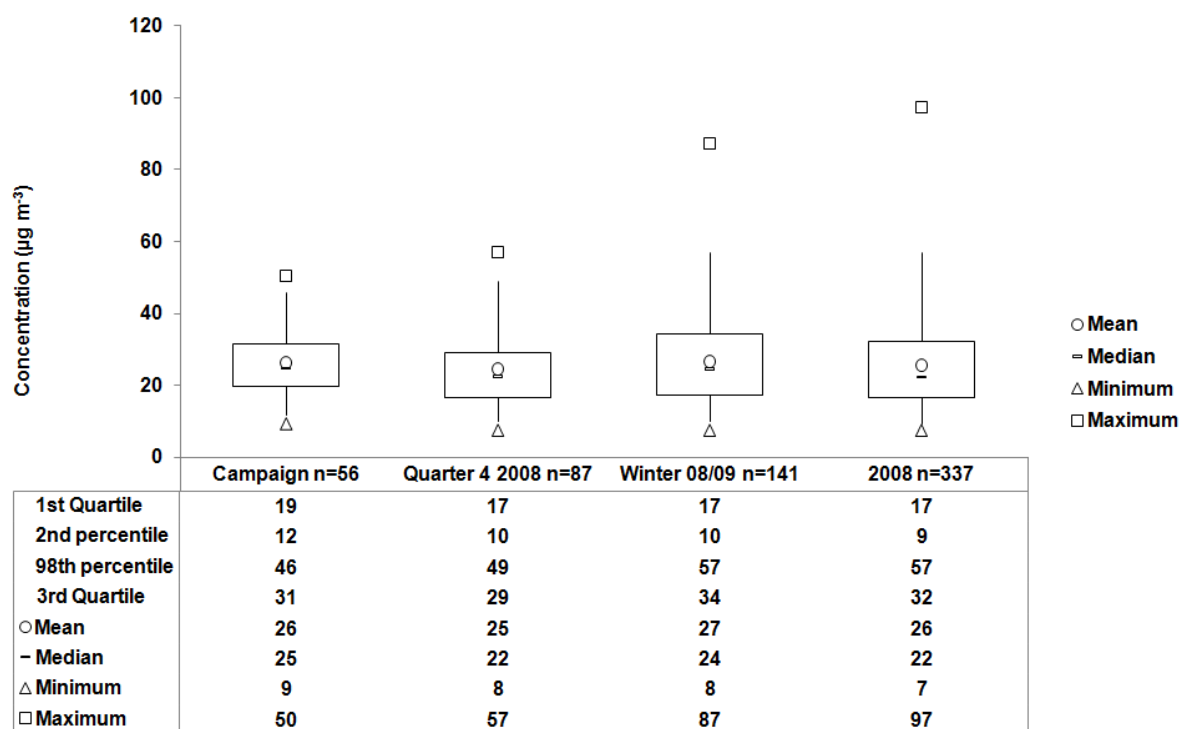|	Campaign n=56	Quarter 4 2008 n=87	Winter 08/09 n=141	2008 n=337
1st Quartile	19	17	17	17
2nd percentile	12	10	10	9
98th percentile	46	49	57	57
3rd Quartile	31	29	34	32
○ **Mean**	26	25	27	26
− **Median**	25	22	24	22
△ **Minimum**	9	8	8	7
□ **Maximum**	50	57	87	97

Figure 3: Summary statistics for PM$_{10}$ measurements during the campaign period, the quarter, the winter and the year

4.1.2. Daily mean concentrations

Due to the design of the experiment and equipment malfunctions not all measurements were made on all days. The single sampler utilised alternate filter media which were analysed for elemental and organic carbon on one day and metals on the other. Key periods of data loss occurred due to the aethalometer between 28th and 30th October, 10th and 24th November and 6th and 11th December.

Daily mean concentrations measured at Swiss Cottage are summarised in Table 1. The results of each metric are discussed in the following sections.

	n	Minimum	1st Quartile	Median	Mean	3rd Quartile	Maximum
PM$_{10}$	43	9.26	19.73	24.76	26.91	31.08	50.33
Elemental Carbon	43	0.79	2.74	4.82	4.45	6.12	8.39
Organic Carbon	24	0.30	1.65	2.29	2.65	3.11	9.36
Aluminium	23	<LOD	0.00	0.00	0.01	0.00	0.12
Barium	23	<LOD	0.00	0.00	0.00	0.01	0.01
Calcium	23	0.02	0.02	0.02	0.12	0.02	1.28
Copper	23	<LOD	0.00	0.01	0.01	0.01	0.01
Iron	23	<LOD	0.00	0.03	0.10	0.09	1.00
Molybdenum	23	<LOD	0.00	0.00	0.00	0.00	0.02
Manganese	23	<LOD	<LOD	<LOD	<LOD	<LOD	<LOD
Sodium	23	0.01	0.13	0.22	0.32	0.33	1.81
Nickel	23	<LOD	0.00	0.00	0.01	0.00	0.10
Lead	23	<LOD	0.00	0.01	0.02	0.02	0.09
Antimony	23	<LOD	0.00	0.00	0.00	0.00	0.01
Strontium	23	<LOD	<LOD	<LOD	<LOD	<LOD	<LOD
Vanadium	23	<LOD	0.00	0.00	0.01	0.00	0.21
Zinc	23	<LOD	0.00	0.00	0.01	0.02	0.07

Table 1: Statistical summary of daily mean concentrations

Note: LOD is limit of detection

4.1.2.1.   PM$_{10}$

Daily mean PM$_{10}$ measurements, calculated from the TEOM using the VCM (as described in section 3.1.1), are shown in Figure 4.The uncertainty shown is expressed at k=2; approximating to two standard deviations; the method of calculating uncertainty is discussed in section 6.
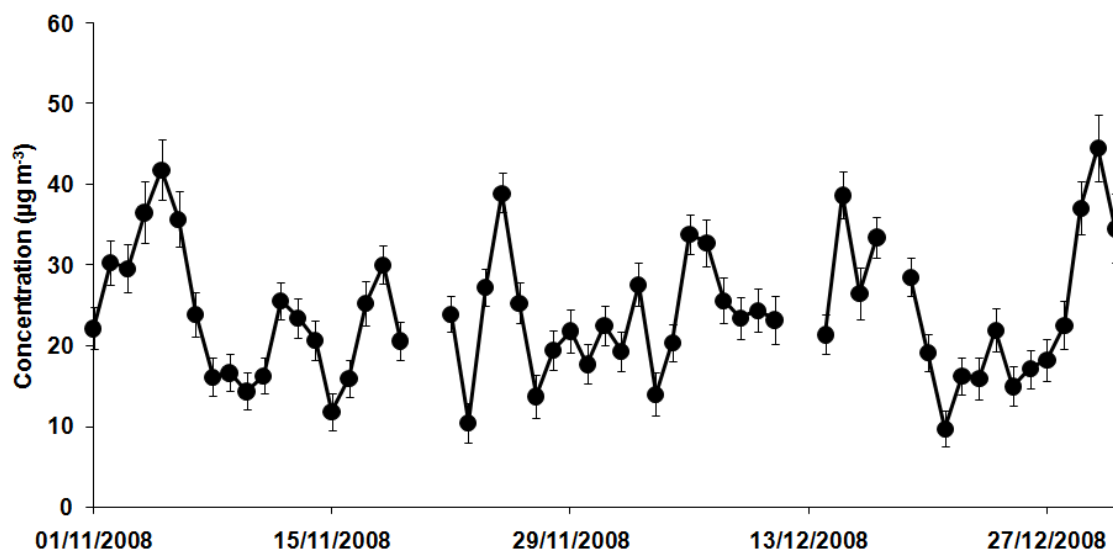

Figure 4: Daily mean VCM PM$_{10}$ measurements

4.1.2.2.   Elemental and black carbon

EC is a by-product of the fuel combustion, it forms small (20-30 nm) spherical particles that agglomerate into clusters up to a few micrometers in size (Seinfeld and Pandis, 1998). EC has been estimated to contribute up to 27 % at roadside sites by Harrison et al. (2003). This form of carbon is very temperature stable, indeed, thermal analysis techniques require temperatures of around 700 ⁰C to pyrolyse it.

Elemental carbon measurements were made directly on filters using the Sunset instrument; as described in section 3.1.3.2. This provided daily mean measurements by chemical analysis but could only be achieved on alternate days due to the need to alternate filter media. Measurements of black carbon were made using the Thermo 8100 Aethalometer; as described in section 3.1.2. This provided 15 minute mean concentrations, which gave an accurate assessment of elemental carbon on the days when the chemical analysis was not undertaken.

To ensure that the results from the Sunset analysis and the aethalometer used in the mass closure analysis were comparable, the days when the Sunset measurements were made alongside the aethalometer measurements were then used to create a set of calibration 'standards' which were used to correct the aethalometer measurements. This was undertaken using Xgenline (http://www.npl.co.uk/mathematics-scientific-computing/software-support-for-metrology/software-support-for-metrology-downloads), which provides generalised distance regression polynomial fitting alongside uncertainties. A time series of elemental carbon concentrations was constructed using the Sunset results interspersed with the adjusted aethalometer results on alternate days; this is shown in Figure 5. The uncertainty shown is expressed at k=2; approximating to two standard deviations; the method of calculating uncertainty is discussed in section 6.
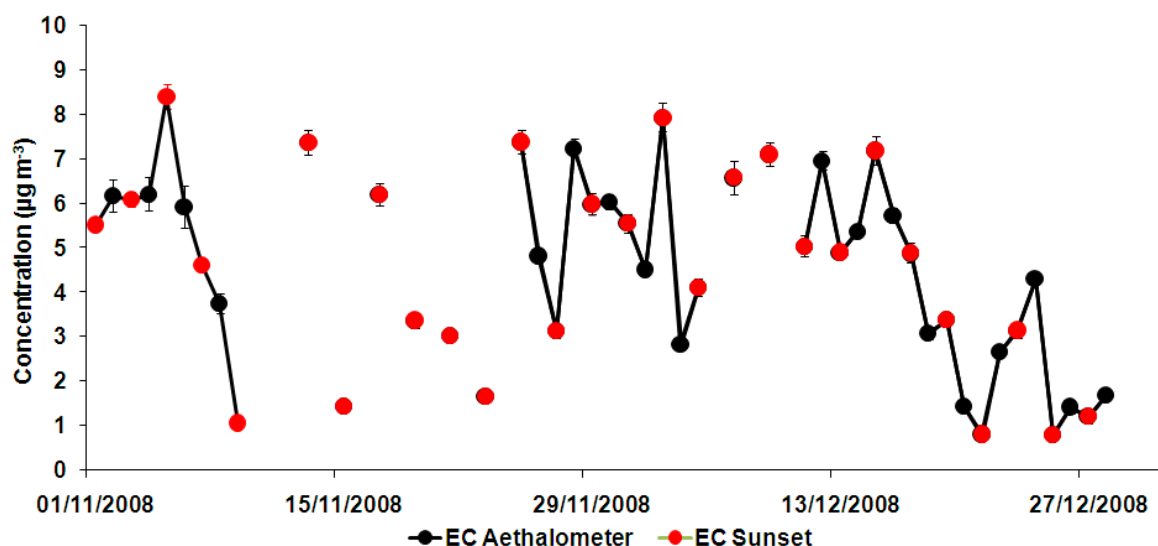
Figure 5: Sunset elemental carbon measurements and aethalometer black carbon measurements

4.1.2.3.   Organic carbon

While elemental carbon is a primary pollutant, emitted directly due to the incomplete combustion of fossil and biomass fuels; organic carbon has both primary and secondary sources. Primary particulate organic carbon is formed during combustion and emitted directly as submicron particles. Other sources include plant spores, pollen, plant debris, tire rubber and soil (Castro et al., 1999). Organic carbon also has secondary sources from gas to particle conversion of volatile organic compounds. This is a result of either condensation of semi-volatile organic species or adsorption onto pre-existing particles (Derwent and Malcolm, 2000; Robinson et al., 2007).

Organic carbon measurements were made directly on filters using the Sunset instrument; as described in section 3.1.3.2. Positive and negative artefacts in OC measurements are well documented (Turpin et al., 2000; Polidori et al., 2006); positive artefacts are accepted to dominate due to the adsorption of organic gases onto the filter and deposited material during sampling. These can be corrected experimentally by sampling using two filters and subtracting the organic carbon measurement on the bottom filter from the measurement on the front filter; this is the quartz-backed-quartz (QBQ) approach. However, due to financial and equipment limitations this method was not feasible in this study. Therefore, in this study, the positive artefact could have either been left in the measurements or estimated and subtracted from the measurements. Several studies have estimated the percentage adsorption of organic gases onto the filter at around 30 % (Turpin et al., 2000; Polidori et al., 2006; Viana et al., 2006; Yttri et al., 2007). Many of these have tended to be away from busy roadside locations such as Swiss Cottage. Studies at urban locations, such as that undertaken in Prague by Schwarz et al. (2008) have suggested that the filter has an adsorption capacity which is reached in urban areas. This is consistent with the offset in the relationship between EC and OC shown in Figure 6. No such offset was found by Harrison et al. (2003), however, that study used filters did not appear to have been pre-fired to remove organic contaminants as recommended in the EMEP draft protocol for EC/OC sampling (EMEP, 2009).

To estimate the concentration that can be attributed to this adsorption, the EC and OC were plotted as a scatter plot, shown in Figure 6 (left). To establish an accurate intercept that was free from artefacts due to the high OC concentrations, 5 % of the measurements with lowest OC concentrations are isolated (these are shown in red) along with 5 % of the measurements with the lowest OC/EC values (shown in blue). The intercept was then established using orthogonal linear regression. The impact of the correction is shown in Figure 6 (right). The corrected OC measurements are shown as a time series in Figure 7. The uncertainty shown is expressed at k=2; approximating to two standard deviations; the method of calculating uncertainty is discussed in section 6. In section 5.1 the organic carbon measurements are apportioned into primary and secondary fractions.
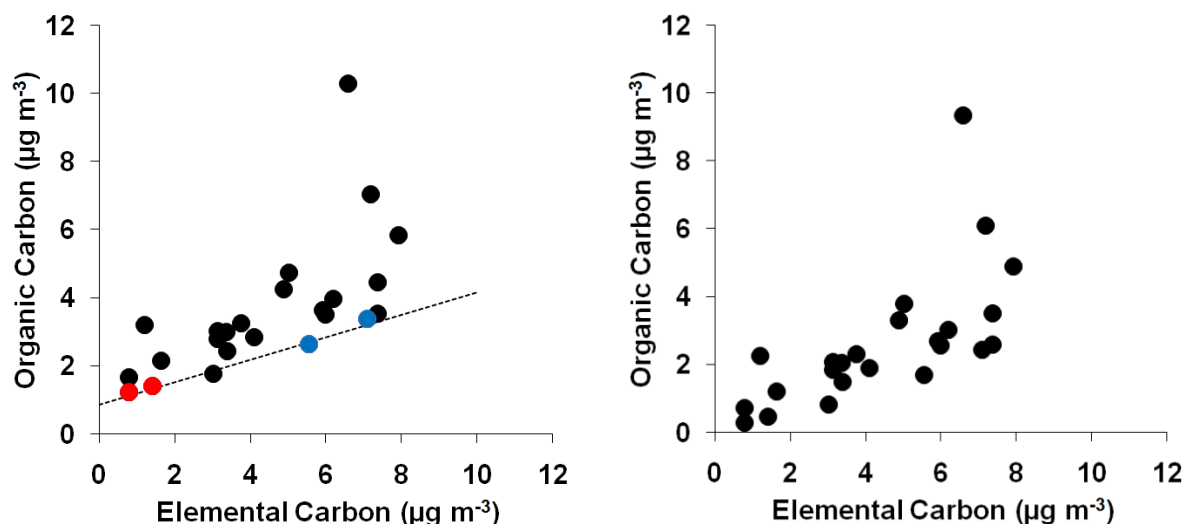
Figure 6: EC and OC measurements before correction for adsorbed gaseous carbon (left) and after correction (right)

Note: Red indicates 5 % of measurements with lowest OC concentrations, blue indicates 5 % of measurements with lowest OC/EC value
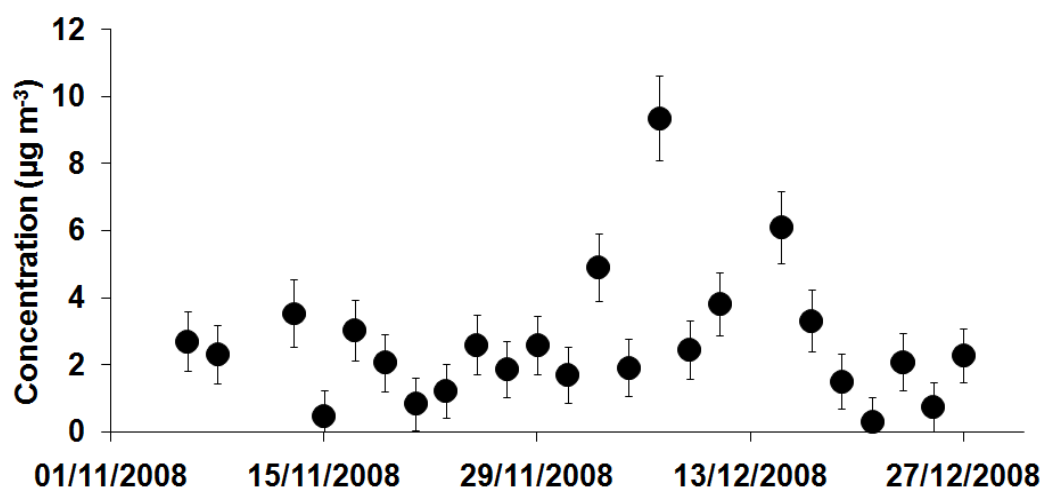

Figure 7: Sunset organic carbon measurements

4.1.2.4.   Metals

Aluminium, Barium, Calcium, Copper, Iron, Molybdenum, Manganese, Sodium, Nickel, Lead, Antimony, Strontium, Vanadium and Zinc concentrations were measured using ICP-MS using the method described in section 3.1.3.4. This chemical analysis could only be achieved on alternate days due to the need to alternate filter media with the Sunset measurements; the daily mean measurements summarised in Figure 3. Twenty-three samples were made and analysed but many are below the limit of detection (LOD), which was assessed as three times the standard deviation of ten acid blanks. Where measurements were below the LOD, a value of 50 % of the LOD has been used. This allowed a mean to be calculated that was not skewed by a small number of high concentrations and also reflected a concentration higher than zero, although in practice all of the LOD's were below 0.04 µg m^{-3} and would therefore have little effect on the mass. The daily mean results are shown as times series in Figure 8, molybdenum and strontium are not shown as all the measurements were below the LOD. The uncertainty shown is expressed at k=2; approximating to two standard deviations; the method of calculating uncertainty is discussed in section 6. The uncertainty cannot be seen on some of the results as it was low enough to be obscured by the data points when plotting.
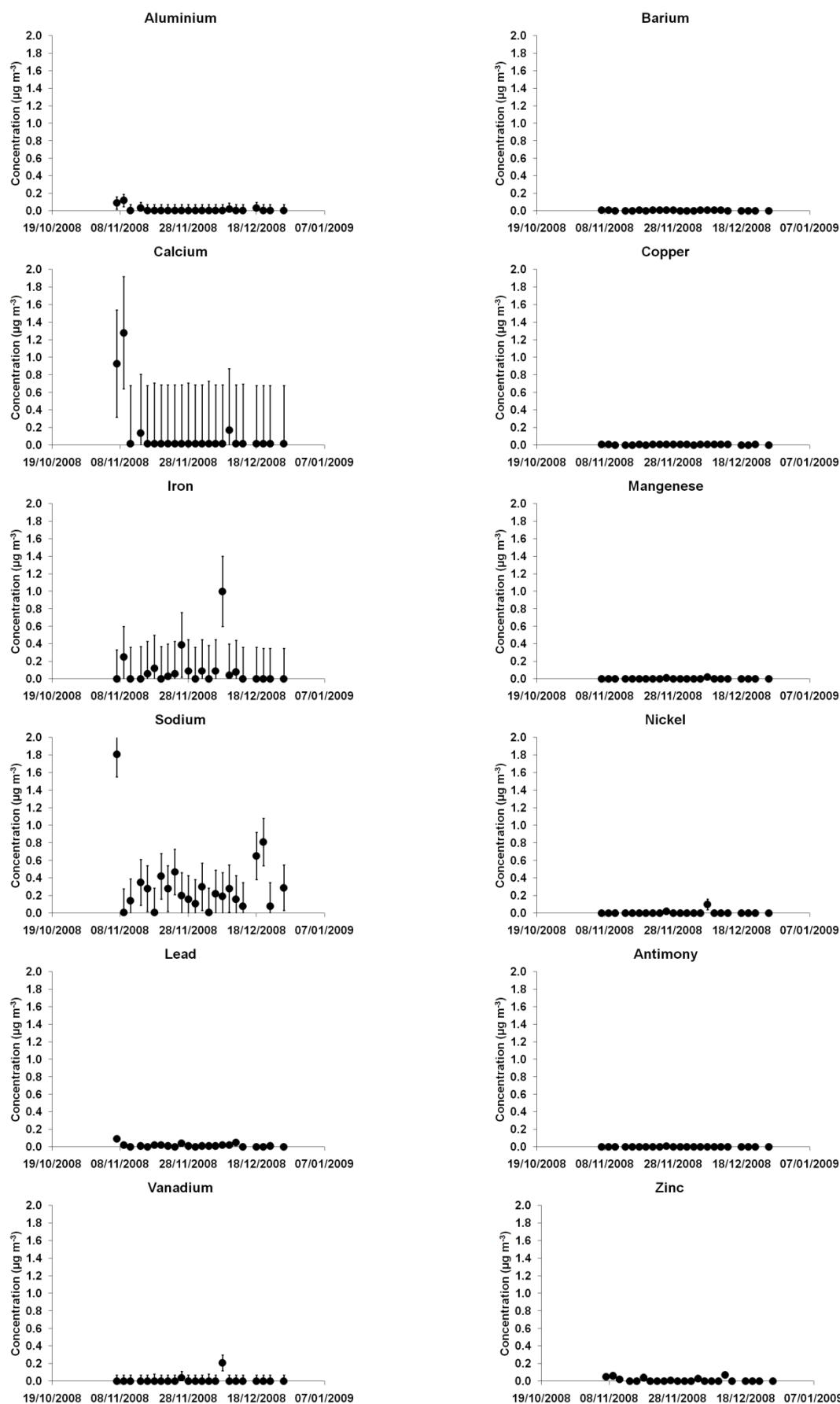
Figure 8: Time series of metal concentrations

5. Mass closure methodology

Mass closure models assess chemical composition by measuring as many of the PM components as possible directly; the remaining mass is estimated based on the knowledge of the chemical composition of these components and any which remain unidentified. This has been achieved using a range of techniques in a number of studies; the relevant methodologies are applied to the measurements available in this study.

The method developed for this study utilised a limited suite of chemical analysis undertaken on samples collected at Swiss Cottage; these focused on PM components which were emitted directly from traffic sources. PM components which have a distant source or are formed by chemical or physical processes which were expected to be uniform over a wide area were measured at the North Kensington background site and the Marylebone Road kerbside site. Each of these provided an element or compound which was then used as a 'marker' of a PM component. As with all mass closure models, assumptions have been made regarding the mass and / or chemical composition of these PM components based on the available literature.

As the sampling methodology only used a single sampler, chemical analysis for metal concentrations and carbon concentrations would only undertaken on alternate days. While the elemental carbon concentrations could be interpolated using the results from the aethalometer and the components of PM which were uniform on a larger scale interpolated from measurements made at other sites, there was no method for interpolating the metals concentrations on the missing days. This results in two sets of data for the mass closure:

- A. Where the full suite of components has been assessed
- B. Where there are no available metals measurements

At each step the uncertainty of the measurement and the uncertainty of the assumption has been combined to provide a standard uncertainty for each PM component at k = 1, which approximates to one standard deviation. These uncertainties have been combined in the final mass closure to provide the uncertainty of the mass closure model at k = 2, which approximates to two standard deviations.
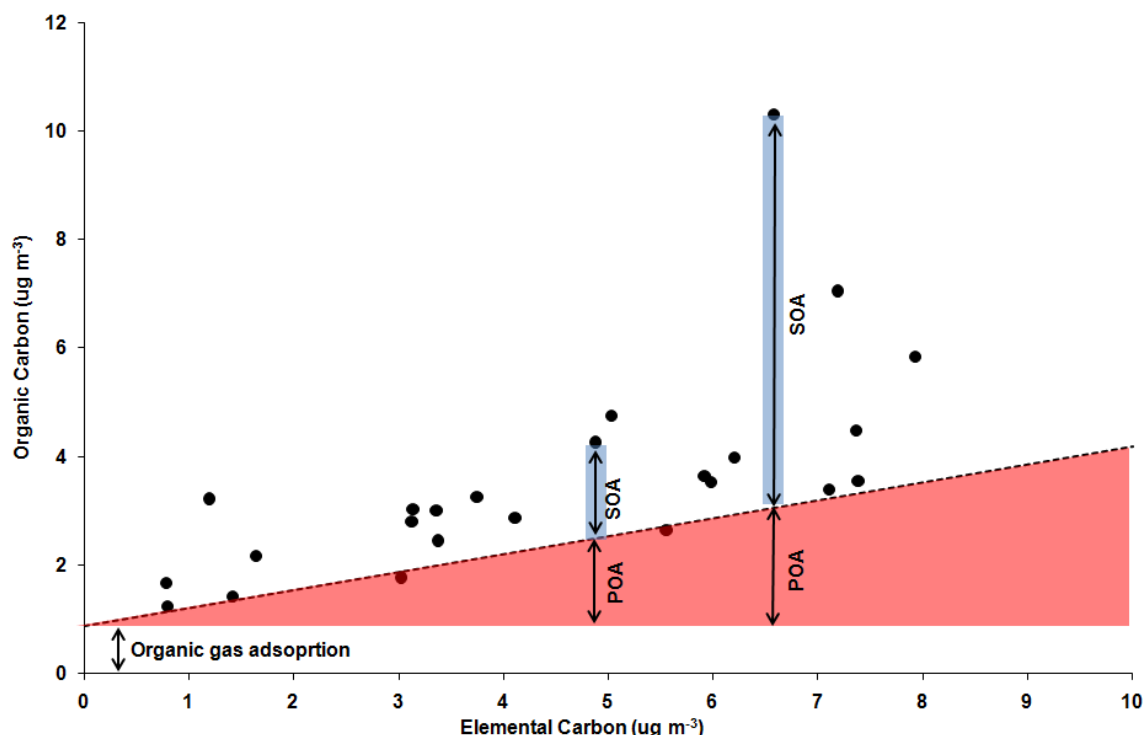
5.1. Elemental Carbon

Elemental carbon concentrations were measured in real time using the aethalometer or on the filters using the Sunset laboratory analysis; the combination of these measurements to provide a unified elemental carbon dataset was described and shown in section 4.1.2.2. These results were used directly in the model; the method of calculating uncertainty is discussed in section 6.

5.2. Primary and Secondary Organic Mass

Organic carbon measurements were apportioned into primary organic aerosol (POA) and secondary organic aerosol (SOA) using the EC tracer method (Polidori et al., 2006) described in Equation 1 and Equation 2; this is also illustrated graphically in Figure 9. This relies on the elemental carbon being a predictor of the POA; the remainder being secondary organic aerosol (SOA). The offset shown in graph relates to the adsorption of gaseous organic components onto the filter, which is removed as described in section 4.1.2.3 The slope of the line (0.33) was used as the $(EC/OC)_{prim}$. This slope is similar to that derived for roadside sites in other studies (Harrison and Yin, 2008; Green et al., 2009).

Equation 1 $SOA = OC - (EC/OC)_{prim} \times EC$

Equation 2 $POA = OC - SOA$

Figure 9: Relationship between elemental and organic carbon measurements

Note: Red area denotes fraction of organic carbon which is primary in origin, blue bars are examples of fraction of organic carbon which is secondary in origin

POA is made up of direct organic gas emissions which form particles through nucleation or condensation (e.g. PAH's) as well as the organic components of soil which may be resuspended by vehicles. SOA is non-traffic related organic compounds which have been oxidised in the atmosphere to form particles or condense onto pre-existing particles; this fraction may also contain organic components from soil which are not traffic related and some components of tyre wear that are traffic related.

POA and SOA were then adjusted to mass concentrations using factors to account for the associated hydrogen and oxygen in the Primary Organic Aerosol Mass (POAM) and the Secondary Organic Aerosol Mass (SOAM). By separating the organic carbon into primary and secondary sources, the different levels of oxidation can be reflected in these factors. The mass of SOA was multiplied by an SOAM factor (*f*SOAM); a value of 2.1 was used. This is the value of organic molecular weight per carbon weight recommended for non-urban aerosol by Turpin and Lim (2001) and was used by Favez et al. (2007), it was considered here to best represent SOAM from long range sources. To account for associated oxygen and hydrogen atoms in the POAM, a *f*POAM of 1.4 was used, this was the measured value from diesel exhaust (Japar et al., 1984).

SOA was assumed to be uniform on a regional scale due to its formation through the oxidation of gaseous organic precursors of both anthropogenic and biogenic origin (Derwent and Malcolm, 2000; Harrison and Yin, 2008). The mean of the SOA concentrations was calculated for the North Kensington and Marylebone Road sites, these were used where measurements from Swiss Cottage was not available; and was termed SOAM$_{regional}$. When the SOAM measurements from Swiss Cottage were compared to the SOAM$_{regional}$, the means of the two datasets were found to be identical (2.1 µg m^{-3}), an orthogonal regression analysis yields a slope of 1.34 (±0.17), an intercept of -0.72 (±0.44) µg m^{-3} and a correlation coefficient of 0.60. The assumption that SOA is uniform therefore appears valid, although there is some uncertainty when comparing the two datasets. This was quantified by examining the standard deviation of the difference between the mean North Kensington and

Marylebone Road measurements and those made at Swiss Cottage during the study period; this was incorporated into the uncertainty calculations described in section 6.

5.3.   Nitrates

Nitrate in PM is predominantly found as ammonium nitrate and sodium nitrate. The former is formed through the oxidation of nitrogen dioxide to nitric acid, which is then neutralised by ammonia. It can exist as either a solid or aqueous solution of NH_4^+ and NO_3^- (Seinfeld and Pandis, 1998). Sodium nitrate is formed when the chlorine in sodium chloride (NaCl) is displaced to the gas phase when it reacts with nitric acid (Seinfeld and Pandis, 1998). This has the effect of transferring nitrate to the aerosol phase and is associated with larger particles resulting in a bimodal distribution of nitrate (Seinfeld and Pandis, 1998).

Both these processes occur on a regional scale and their concentrations are assumed to be regional across London. The oxidation of nitrogen dioxide to nitric acid and its subsequent neutralisation occurs in a number of hours, this can lead to an urban increment in ammonium nitrate. However, little evidence of a difference between roadside and background concentrations of ammonium nitrate has been found in London during previous studies (Harrison et al., 2004).

The nitrate concentration in PM$_{10}$ was measured at North Kensington and Marylebone Road as part of Defra's Particle Concentrations and Numbers Network; the methodology is described in section 3.1.3.3. The mean of these measurements was used a regional nitrate concentration. The uncertainty associated with applying the measurements at one location to another was quantified by examining the standard deviation of the difference between the measurements made at North Kensington and Marylebone Road during a reference period (1st August 2006 – 31st December 2006); this was incorporated into the uncertainty calculations described in section 6.

As only measurements of nitrate were made, it is impossible to differentiate between ammonium and sodium nitrate to provide a total nitrate mass NO$_{3total}$. Other studies have achieved this differentiation either by analysing a full suite of ions (White, 2008) or by measuring fine and coarse PM and assuming that ammonium nitrate is in the former and sodium nitrate in the later (Harrison et al., 2003). As the mass associated with the cations (ammonium (18) and sodium (23)) is very similar, an estimate of the factor to be applied (fNO$_3$) can be made. This estimate is based on the study by Harrison (2003) in London, which found that approximately 60 % of nitrate was found in the fine fraction and could therefore be assumed to be ammonium nitrate; an fNO$_3$ of 1.32. The uncertainty in the relative abundance of these compounds could then be incorporated in the uncertainty described in section 6.

5.4.   Sulphates

Sulphate in PM is found mostly as ammonium sulphate, although it can also be present as ammonium bisulphate (NH_4HSO_4). These are predominately in the fine fraction due to the homogeneous nucleation route of sulphate particle formation (Harrison et al., 2004). Clarke et al. (1999) also identified a second peak in size distribution between 3 μm and 6 μm which they assigned to metal sulphates such as gypsum ($CaSO_4.2H_2O$).

As the difference in mass ratio between the ammonium ion in ammonium sulphate and ammonium bisulphate and the calcium and water in gypsum is so large, it is difficult to represent this as a mean fSO$_4$. Furthermore, the mass of gypsum is accounted for later in section 5.7. A fSO$_4$ of 1.19 was therefore used to account for the mass of ammonium in ammonium sulphate; no adjustment has been made for ammonium bisulphate as this was expected to be less abundant. This was the methodology used by Frank (2006) although Harrison (2003) first accounted for the sulphate in gypsum.

The sulphate concentration in PM$_{10}$ was measured at North Kensington and Marylebone Road as part of Defra's Particle Concentrations and Numbers Network; the methodology is described in section 3.1.3.3. The mean of these measurements was used as a regional sulphate concentration. The uncertainty associated with applying the measurements at one location to another was quantified by

examining the standard deviation of the difference between the measurements made at North Kensington and Marylebone Road during a reference period (1st August 2006 – 31st December 2006); this was incorporated into the uncertainty calculations described in section 6.

5.5. Chlorides

Chloride in PM is found mostly as sodium chloride, which is formed from sea spray (Seinfeld and Pandis, 1998); highest concentrations are found at coastal locations (White, 2008). Road salting during winter is another source (Harrison and Jones, 1995; Clarke et al., 1999). It can also be present as ammonium chloride and hydrogen chloride, indeed Jones and Harrison (2009) have estimated that 35 - 45 % of chloride is not from marine sources. Nevertheless, until further evidence is available chloride is assumed to be all sodium chloride, as it was by Harrison et al. (2003). An ƒCl of 1.65 is therefore used to account for the associated mass of sodium.

The chloride concentration in PM$_{10}$ was measured at North Kensington and Marylebone Road as part of Defra's Particle Concentrations and Numbers Network; the methodology is described in section 3.1.3.3. The mean of these measurements was used a regional chloride concentration. The uncertainty associated with applying the measurements at one location to another was quantified by examining the standard deviation of the difference between the measurements made at North Kensington and Marylebone Road during a reference period (1st August 2006 – 31st December 2006); this was incorporated into the uncertainty calculations described in section 6.

5.6. Water

Water is associated with hygroscopic species such as nitrate, sulphates and some organic species; it is retained in the PM due to the incomplete removal at the measurement relative humidities. Harrison et al. (2003) estimated this at 29 % of the mass of ammonium nitrate and ammonium sulphate based on a regression analysis between the TEOM and reference PM$_{10}$ measurements. This has also been assessed using the AIM model by Frank (2006). This study has repeated the work of Frank (2006) and used the AIM model (Clegg et al., 2009) to assess the concentration of water associated with the PM.

The AIM model was accessed through its web site (http://www.aim.env.uea.ac.uk/aim/aim.php); the chemical inputs are NO_3^-, SO_4^{2-}, NH_4^+ and H^+ ions. The model environment was set to be 30 ºC and 30 % RH which reflects the operating environment of the FDMS, which the TEOM$_{VCM}$ most resembles. The NO_3^-, SO_4^{2-} ions were measured directly as described in section 3.1.3.3. The NH_4^+ ion concentration was estimated based on 60 % of the NO_3^- being associated with NH_4^+ in ammonium nitrate. The remaining H^+ ions are used to balance the charge.

5.7. Minerals

The mineral composition of PM comes from windblown dust from soil and roadside verges, construction activity and spilt loads as well as its potential resuspension of this material by traffic. The mineral content of PM is therefore a complex, multi-component fraction which is challenging to assess. The key elemental components of crustal rock are oxygen, silicon, aluminium, iron and calcium, while in soils they are oxygen, silicon, aluminium, iron and carbon. Primary (un-weathered) minerals include quartz (SiO_4) and more complex silicates such as olivines (iron rich) and feldspars (aluminium rich). Secondary (weathered) minerals include gibbite ($Al(OH)_3$), hematite (Fe_2O_3), calcite ($CaCO_3$) and gypsum ($CaSO_4.2H_2O$) (Sposito, 1989).

Harrison et al. (2003) used iron measured in the PM$_{coarse}$ as a marker for vehicle and soil dust, which was correlated against the unidentified mass to achieve mass closure as 'iron-rich dust'. Frank (2006) used an equation using silicon, calcium, iron and titanium to apportion crustal material. Of the metallic elements measured in this study, aluminium and calcium occur in sufficient quantities to be used as tracers for mineral dusts.

5.7.1. *Feldspars*

Aluminium has been chosen as a tracer for feldspars. Factors have been derived for the end members (purest forms) of the three common classes of feldspars (potassium feldspar (KAlSi$_3$O$_8$), , albite (NaAlSi$_3$O$_8$) and anorthite (CaAl$_2$Si$_2$O$_8$)) to account for the mass of potassium, sodium, calcium, silicon and oxygen in these minerals. A mean ƒAl of 8.40 was calculated. The uncertainty in this factor been incorporated in the uncertainty described in section 6.

5.7.2. *Calcium compounds*

Calcium has been chosen as a tracer for weathered minerals such as calcite and gypsum, as well as being present in other minerals such as feldspars. Factors have been derived for both calcite and gypsum to account for the mass of associated carbonate and sulphate ions and the water associated with gypsum. A mean ƒCa of 3.80 was derived. The uncertainty in this factor been incorporated in the uncertainty described in section 6.

5.8.   Iron oxide

The other metal measured in PM$_{10}$ in sufficient quantity to impact on the PM$_{10}$ was iron. This was used by Harrison et al. (2003) as a tracer for a vehicle and soil derived component termed 'iron-rich dust'. Iron measured in the PM$_{coarse}$ fraction was regressed against the unidentified mass and a factor was optimised to best represent this missing mass. In this study, as aluminium and calcium have been used as direct tracers for minerals, iron is therefore assumed to be present as an oxide (FeO, Fe$_2$O$_3$ or Fe$_3$O$_4$) both from mineral and vehicular sources (brake wear and corrosion). Factors have been derived for all three oxides; a mean of 1.37 was therefore used to represent the oxygen associated with the iron measured.

5.9.   Other metals

The concentrations of the other metals (barium, copper, molybdenum, manganese, nickel, lead, antimony, strontium, vanadium and zinc) were very low and therefore contribute little to the PM$_{10}$ mass; their masses have been summed. Although sodium was measured, its mass was accounted for as part of the mass of sodium nitrate, sodium chloride and as a component of the feldspars. The uncertainty calculation is described in section 6.

5.10.   Unidentified mass

As the sampling methodology only used a single sampler, this results in two sets of data for the mass closure:

   A.   Where the full suite of components has been assessed
   B.   Where there are no available metals measurements

For dataset A the mass closure method results in a reconstructed mass concentration that was either greater or less than the measured PM$_{10}$ mass.

However, dataset B has known missing components; the magnitude of these components (and the uncertainty in this value) can be calculated by examining the difference between the measured PM$_{10}$ mass and the incomplete suite of components (see section 6). This provides a mass closure with a quantified but unidentified mass.

6. Uncertainty

The uncertainty was calculated using the GUM methodology (ISO, 1995). This approach requires several steps:

1. Establishment of a model or measurement equation which represents the procedure for obtaining the desired output quantity from the input quantities.
2. Identification and quantification of all individual sources of uncertainty.
3. Combination of the individual uncertainties to obtain a combined standard uncertainty (u_c).
4. Calculation of the expanded uncertainty U, by multiplying u$_c$ by the coverage factor k.

As shown in section 5, the mass closure model has many steps and many inputs; these have been assessed component-by-component and combined in a final model uncertainty. The uncertainty in the PM$_{10}$ concentrations has been assessed independently using the same methodology and is expressed at k = 2. All the component uncertainties are expressed at k = 1 except uncertainty in the total mass, which is expressed at k = 2.

6.1. PM$_{10}$

The TEOM$_{VCM}$ measurements are calculated using Equation 3. The uncertainty in the TEOM$_{VCM}$ is then described in Equation 4.

Equation 3 $TEOM_{VCM} = TEOM – (fVCM \times FDMS\ purge) – FDMS\ purge$

Equation 4 $UVCM = 2 \times \sqrt{(uTEOM)^2 + (ufVCM \times FDMS\ purge)^2 + (fVCM \times uFDMS\ purge)^2}$

Where:

fVCM is the VCM factor, calculated as 0.87 (Green et al., 2009)

FDMS purge is the mean of the FDMS purge measurements from the three closest monitoring sites

uTEOM is the uncertainty in the TEOM measurements

ufVCM is the uncertainty in the VCM factor, calculated as 0.2 (Green et al., 2009)

uFDMS is the uncertainty in the FDMS purge measurements

6.2. Elemental carbon

The EC measurements are calculated using Equation 5. Equation 6 shows the uncertainty equation for EC. The EC blank value was zero and was therefore not incorporated into the uncertainty equation.

Equation 5 $EC = (EC_m \times a)/V - (EC_b \times a)/V$

Where:

EC$_m$ is measured Elemental Carbon

EC$_b$ is measured Elemental Carbon in blank

a is the 1/fraction of the filter analysed

V is the volume

Equation 6 $uEC = \sqrt{((uEC_m \times -a)^2 / V^2 + (EC^2 \times uf^2) / 100^2)}$

Where:

EC is the elemental carbon concentration

uEC$_m$ is the uncertainty in the EC measurement

uf is the uncertainty in flow as a percentage

6.3.   Primary and secondary organic carbon

The uncertainty calculations for POAM and SOAM rely on inputs from a number of sources including the OC and EC measurements and the ƒPOAM and ƒSOAM. OC was measured in a similar way to EC, the measurements are calculated using Equation 7. Equation 8 shows the uncertainty equation for OC.

Equation 7   *OC = (OC$_m$ x a)/V - (OC$_b$ x a)/V - c*

Where:

OC$_m$ is measured Elemental Carbon

OC$_b$ is measured Elemental Carbon in blank

a is the 1/fraction of the filter analysed

V is the volume

C is the intercept derived from the analysis in section 4.1.2.3.and represents the adsorbed organic gases

Equation 8   *uOC = √((uOC$_m$ x -a)^2 / V^2 + (uOC$_b$ x -a)^2 / V^2 + (OC^2 x uf^2) / 100^2) + uc^2)*

Where:

OC is the organic carbon concentration

uOC$_m$ is the uncertainties in the ambient EC measurement

uOC$_b$ is the uncertainties in the EC blank measurement

uf is the uncertainty in flow as a percentage

uc is the uncertainty in the intercept derived from the analysis in section 4.1.2.3

The uncertainty in the SOAM was calculated using Equation 9

Equation 9   *uSOA = √(uOC^2 + (u(EC / OC)$_{prim}$ x EC)^2 + ((EC / OC)$_{prim}$ x uEC)^2)*

Where:

uOC was calculated from Equation 7

u(EC/OC)prim is the uncertainty in the slope shown in Figure 6

The regional SOA, derived from the mean of the Marylebone Road and North Kensington measurements, has an additional uncertainty to reflect the difference between measurements at Swiss Cottage and the other sites. This has been estimated by calculating the standard deviation of the difference between the SOAregional and the SOA at Swiss Cottage; a value of 1.24 µg m^{-3} was used in Equation 11.

Equation 10   *uSOA$_{regional}$ = √(uSOA^2 + uSOA$_{regional}$^{2})*

The estimation of the oxygen and hydrogen atoms associated with the SOA also has some uncertainty. Turpin and Lim (2001) evaluated these ratios and recommended 2.1 (±0.2); 0.2 is therefore used as the uSOAM in Equation 11 to provide an uncertainty for SOAM.

Equation 11   *uSOAM = √(uSOA x ƒSOAM)^2 + (SOA x ufSOAM)^2*

The uncertainty in the POAM was calculated from Equation 12 and Equation 13. As ƒPOAM was a measured quantity by Japer et al. (1984), its uncertainty was assumed for these purposes to be zero.

Equation 12   *uPOA = √(uOC^2 + uSOA^2)*

Equation 13   *uPOAM = √((uPOA x ƒPOAM)^2 + (SOA x ufPOAM)^2)*

6.4.   Nitrates

The regional nitrate, derived from the mean of the Marylebone Road and North Kensington measurements, has an additional uncertainty to reflect the application of measurements from another site to Swiss Cottage. This has been estimated by calculating the standard deviation of the difference

between the North Kensington and Marylebone Road sites (0.53 μg m^{-3}) and is incorporated in the uncertainty equation in Equation 14.

Equation 14 $uNO_{3regional} = \sqrt{(} (uNO_3)^2 + (uNO_{3regional})^2)$

Where:

uNO$_3$ is the reported uncertainty in the analysis (4.5% of measured value) (Yardley et al., 2007b)

uNO$_{3regional}$ is the standard deviation of the difference between North Kensington and Marylebone from 2006

The uncertainty in the fNO$_3$ has been calculated by increasing the relative abundance of ammonium nitrate and then sodium nitrate by 25 % from the 60 % starting point and calculating a new fNO$_3$. This results in a minimum fNO$_3$ of 1.30 and a maximum fNO$_3$ of 1.34; this has then been incorporated into the uncertainty equation in Equation 15.

Equation 15 $uNO_{3total} = \sqrt{(} (uNO_{3regional} \times fNO_3)^2 + (NO_{3regional} \times ufNO_3)^2)$

6.5.   Sulphates

The regional sulphate, derived from the mean of the Marylebone Road and North Kensington measurements, has an additional uncertainty to reflect the application of measurements from another site to Swiss Cottage. This has been estimated by calculating the standard deviation of the difference between the North Kensington and Marylebone Road sites (0.35 μg m^{-3}) and is incorporated in the uncertainty equation in Equation 14.

Equation 16 $uSO_{4regional} = \sqrt{(} (uSO_4)^2 + (uSO_{4regional})^2)$

Where:

uSO$_4$ is the reported uncertainty in the analysis (4.5% of measured value) (Yardley et al., 2007b)

uSO$_{4regional}$ is the standard deviation of the difference between North Kensington and Marylebone from 2006

As there is assumed to be no uncertainty in the fSO$_4$, the uncertainty equation (Equation 17) for uSO$_{4total}$ is simpler.

Equation 17 $uSO_{4total} = \sqrt{((}uSO_{4egional} \times fSO_4)^2$

6.6.   Chloride

The regional chloride, derived from the mean of the Marylebone Road and North Kensington measurements, has an additional uncertainty to reflect the application of measurements from another site to Swiss Cottage. This has been estimated by calculating the standard deviation of the difference between the North Kensington and Marylebone Road sites (0.30 μg m^{-3}) and is incorporated in the uncertainty equation in Equation 14.

Equation 18 $uCl_{regional} = \sqrt{(} (uCl)^2 + (uCl_{regional})^2)$

Where:

uCl is the reported uncertainty in the analysis (4.5% of measured value) (Yardley et al., 2007b)

uCl$_{regional}$ is the standard deviation of the difference between North Kensington and Marylebone from 2006

As there is assumed to be no uncertainty in the fCl, the uncertainty equation (Equation 19) for uCl$_{total}$ is again simple.

Equation 19 $uCl_{total} = \sqrt{((}uCl_{regional} \times fCl)^2$

6.7.   Water

The uncertainty in the AIM model results is composed of both an uncertainty in the AIM model predictions and an uncertainty in the model inputs; these are combined in Equation 20.

Equation 20

$$uWater = \sqrt{\begin{array}{c}(uAIM \times H_2O)^2 + \left(\dfrac{uSO_4 \times H_2O \times SO_4}{\sum SO_4 + NO_3 + NH_4 + H}\right)^2 + \left(\dfrac{uNO_3 \times H_2O \times NO_3}{\sum SO_4 + NO_3 + NH_4 + H}\right)^2 + \\ \left(\dfrac{uNO_3 \times H_2O \times NH_4}{\sum SO_4 + NO_3 + NH_4 + H}\right)^2 + \left(\dfrac{uH \times H_2O \times H}{\sum SO_4 + NO_3 + NH_4 + H}\right)^2\end{array}}$$

Where:

uAIM is the estimated uncertainty in the model output (5 %) from the uncertainty in the solubility constant of ammonium nitrate and ammonium sulphate

H$_2$O, SO$_4$, NO$_3$, NH$_4$ and H are the measured values of H$_2$O, SO$_4$, NO$_3$, NH$_4$ and H respectively

uSO$_4$, uNO$_3$, uNH$_4$ and uH are the uncertainties in the SO$_4$, NO$_3$, NH$_4$ and H measurements respectively

6.8.   Metals

The uncertainty in the metal concentrations was calculated using Equation 22. This was derived from Equation 21, which was used to determine metal concentrations from the ICP-MS analysis.

Equation 21 $M = (M_m \; x \; V_d \; x \; A_p) \; / \; V_s$

Where:

M is the final metal concentration

M$_m$ is the measured concentration on the filter

V$_d$ is the volume of the final digested solution

A$_p$ is the area of the punch relative to the whole filter

V$_s$ is the volume of air sampled onto the whole filter

Equation 22

$$uM = \sqrt{\frac{(uM_m \times V_d \times -A_p)^2}{V_s{}^2} + \frac{(-M_m \times uV_d \times A_p)^2}{V_s{}^2} + \frac{(M_m \times -V_d \times uA_p)^2}{V_s{}^2} + \frac{M^2 \times uf^2}{100^2}}$$

Where:

uM$_m$, uV$_d$ and uA$_p$ are the uncertainties in M$_m$, V$_d$ and A$_p$ respectively

uf is the uncertainty in flow as a percentage

6.8.1.   Minerals

The uncertainty in the fAl has assessed as the standard deviation in the fKAlSi$_3$O$_8$, fNaAlSi$_3$O$_8$ and fCaAl$_2$Si$_2$O$_8$; this was 2.82 and has then been incorporated into the uncertainty equation in Equation 26.

Equation 23   *uFeldspar = √((uAl x fAl)^2 + (Al x ufAl)^2)*

Where

uAl is the calculated measurement uncertainty for Al

ufAl is the standard deviation of the fKAlSi$_3$O$_8$, fNaAlSi$_3$O$_8$ and fCaAl$_2$Si$_2$O$_8$

The uncertainty in the fCa has assessed as the standard deviation in the fCaCO$_3$ and fCaSO$_4$.2H$_2$O; this was 1.14 and has then been incorporated into the uncertainty equation in Equation 26.

Equation 24   *uCalcium Compounds = √((uCa x fCa)^2 + (Ca x ufCa)^2)*

Where

uCa is the calculated measurement uncertainty for Ca

uCa is the standard deviation of the ƒCaCO$_3$ and ƒ CaSO$_4$.2H$_2$O

The uncertainty of the minerals is a combination of these two uncertainties and is shown in Equation 25.

Equation 25 $uMinerals = \sqrt{(uCalcium\ Compounds)^2 + (uFeldspar)^2}$

6.8.1.1.   Iron oxide

The uncertainty in the ƒFe has assessed as the standard deviation in the ƒFe's of FeO, Fe$_2$O$_3$ and Fe$_3$O$_4$; this was 0.07 and has then been incorporated into the uncertainty equation in Equation 26.

Equation 26 $uIronOxide = \sqrt{(uFe \times fFe)^2 + (Fe \times ufFe)^2}$

Where

uFe is the calculated measurement uncertainty for Fe

ufFe is the standard deviation of the ƒFe's of FeO, Fe$_2$O$_3$ and Fe$_3$O$_4$

6.8.2.   Other metals

The uncertainty in the concentrations of the other metals was calculated using Equation 27.

Equation 27 $uMetals = \sqrt{uAl^2 + uBa^2 + uCu^2 + uMn^2 + uMo^2 + uNi^2 + uPb^2 + uSb^2 + uSr^2 + uV^2}$

6.8.3.   Unidentified Mass

The uncertainty of the unidentified mass is calculated from the sum of the uncertainty of PM$_{10}$ and the sum of the uncertainties in all components excluding those derived from the metals measurements; this is shown in Equation 28.

Equation 28 $uUnidentifiedMass = \sqrt{uPM_{10}^2 + uEC^2 + uPOAM^2 + uSOAM^2 + uNitrates^2 + uSulphates^2 + uChlorides^2 + uWater^2}$

6.8.4.   Total PM$_{10}$ Mass

The uncertainty of the reconstructed mass is calculated by combining all of the uncertainties of the components and then multiplying by a coverage factor (k) of 2. As different components contribute to data sets A and B, they will have different uncertainty equations; these are shown in Equation 29 and Equation 30 respectively.

Equation 29 $uTotalMassA = 2x\ \sqrt{uEC_a^2 + uPOAM_a^2 + uSOAM_{regional}^2 + uNO_{3total}^2 + uSO_{4total}^2 + uCl_{total}^2 + uWater^2 + uMinerals^2 + uIronOxide^2 + uMetals^2}$

Where:

uEC$_a$ is the uncertainty in the EC measurements from the aethalometer

uPOAM$_a$ is the uncertainty in the EC measurements generated from the EC$_a$

Equation 30 $uTotalMassB = 2x\ \sqrt{uEC_s^2 + uPOAM_s^2 + uSOAM^2 + uNO_{3total}^2 + uSO_{4total}^2 + uCl_{total}^2 + uWater^2 + uUnidentified^2}$

Where:

uEC$_s$ is the uncertainty in the EC measurements from the aethalometer

uPOAM$_S$ is the uncertainty in the POAM measurements generated from the EC$_s$

7. Mass closure results and discussion

This section reports the results of the mass closure model, explores the relationships with the measured PM$_{10}$ concentrations and the implication of the uncertainty in the model.

7.1. Daily mean concentrations

Due to the design of the experiment and equipment malfunctions not all measurements were made on all days. The single sampler utilised alternate filter media which were analysed for elemental and organic carbon on one day, which were converted to POAM and SOAM concentrations, and metals, which were converted to mineral and metal oxide concentrations, on the other. Regional components were calculated from the mean of the available measurements from Marylebone Road and North Kensington. As discussed in section 5.10, this leads to the production of two datasets (A and B); one with a full suite of chemical components and one which is missing the mineral, iron oxide and metal components. Daily mean concentrations measured at Swiss Cottage are summarised in Table 2 and displayed as a time series in

.

	Dataset	n	Minimum	1st Quartile	Median	Mean	Mean %	3rd Quartile	Maximum
PM$_{10}$	A	11	16.6	18.3	21.5	21.7	-	24.3	28.2
	B	32	9.3	21.6	28.2	28.7	-	34.2	50.3
EC	A	11	1.1	2.0	4.5	3.8	18.4%	5.1	7.2
	B	32	0.8	3.1	5.3	4.7	18.5%	6.2	8.4
POAM	A	11	0.5	0.9	2.1	1.8	8.5%	2.4	3.3
	B	32	0.4	1.4	2.4	2.2	8.6%	2.9	3.9
SOAM	A	11	0.7	1.7	2.7	3.2	15.3%	4.2	7.8
	B	32	-0.3	1.1	2.0	2.8	11.0%	3.8	13.7
Nitrates	A	11	0.0	2.9	3.7	3.7	17.6%	4.9	7.3
	B	32	1.2	3.7	6.2	6.4	25.3%	8.0	15.7
Sulphates	A	11	0.9	1.5	1.7	2.3	11.1%	2.9	6.0
	B	32	0.8	1.3	2.1	2.3	9.3%	3.1	7.4
Chlorides	A	11	2.0	2.5	3.7	3.6	17.6%	4.3	6.7
	B	32	1.0	2.7	4.0	3.9	15.6%	4.7	8.7
Water	A	11	0.0	0.8	1.0	1.3	6.1%	1.6	4.0
	B	32	0.0	0.2	0.9	1.2	4.9%	1.6	5.0
Minerals	A	11	0.1	0.1	0.1	1.0	4.8%	0.1	5.9
	B	-	-	-	-	-	-	-	-
Iron oxide	A	11	0.0	0.0	0.0	0.1	0.5%	0.1	0.5
	B	-	-	-	-	-	-	-	-
Other metals	A	11	0.0	0.0	0.0	0.0	0.2%	0.1	0.2
	B	-	-	-	-	-	-	-	-
Unidentified	A	11	-4.1	-2.3	-1.0	-0.3	-1.3%	1.2	6.1
	B	32	-6.2	-0.3	0.8	1.7	6.7%	3.2	11.1
Total mass	A	11	8.4	17.3	19.0	20.8	100.0%	22.6	31.5
	B	32	10.9	20.9	26.5	25.2	100.0%	30.6	49.5

Table 2: Statistical summary of daily mean PM$_{10}$ component concentrations

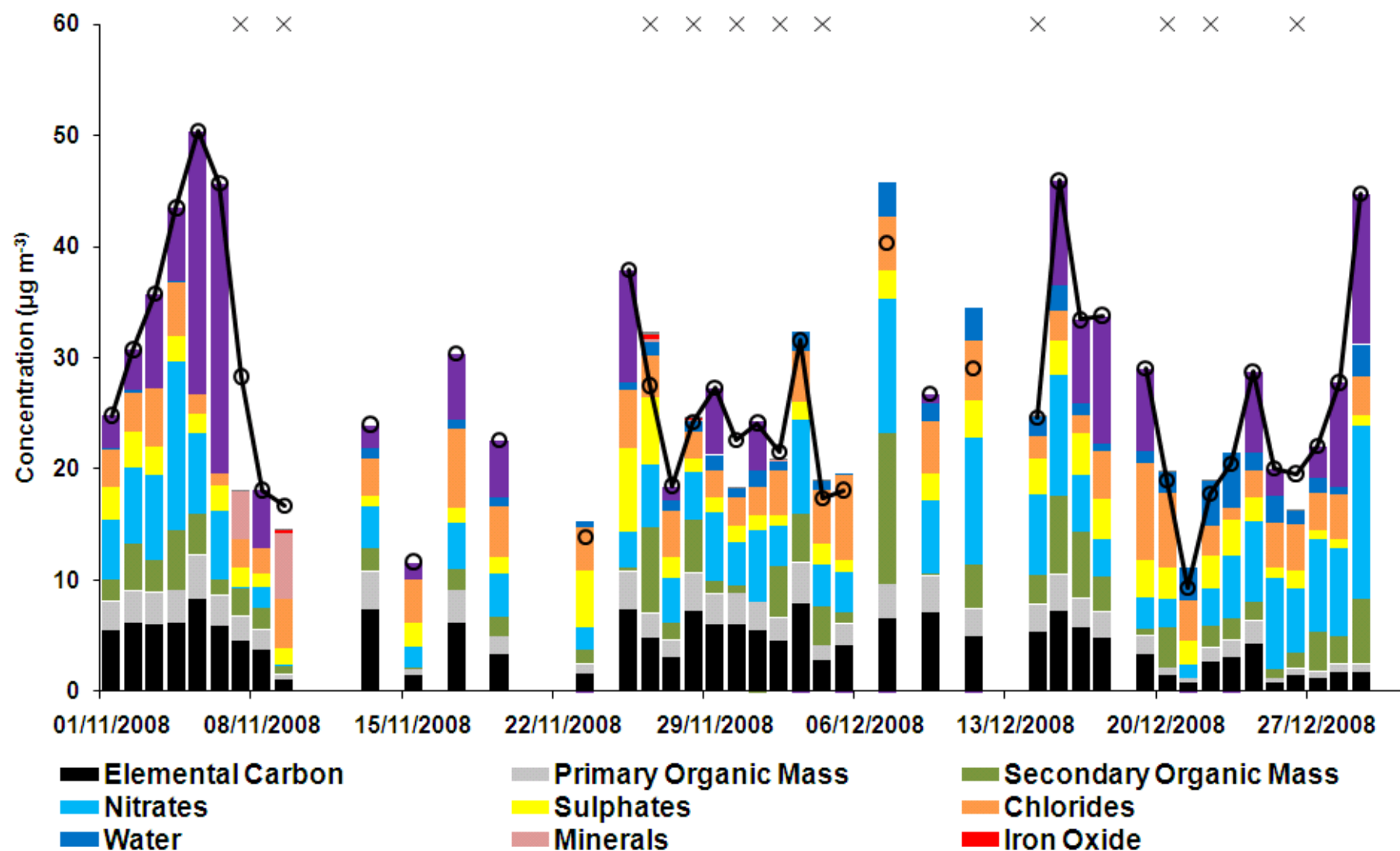*Note: Total mass A does not include the unidentified mass, while total mass B does include the unidentified mass*

Figure 10: Time series of PM components compared to PM$_{10}$ mass for both datasets A and B

Note: Days in dataset A are marked with an X

7.2. Dataset A

Key periods of data loss occurred due to the aethalometer between 28th and 30th October, 10th and 24th November and 6th and 11th December. Data loss also occurred when the TEOM malfunctioned on 12th and 18th December. Together, this resulted in a reduction in the number of samples available to dataset A, which relies on these measurements, from the planned 30 to 11.

The mean chemical composition of the samples in dataset A is shown in Figure 11 (left). Elemental carbon concentrations contributed 18 % to the mass while the organic fraction contributed 23 % to the mass, split 8 % primary and 15 % secondary. Sulphate salts contributed 11 % while the nitrate, chloride both made up 18 % of the total mass. The water associated with these components added a further 6 %. The remaining 6 % of the mass was comprised of minerals, iron oxide and other metals. On average the reconstructed mass was 0.3 µg m^{-3} larger than the measured mass; this varied between -4.1 µg m^{-3} and +6.1 µg m^{-3}.
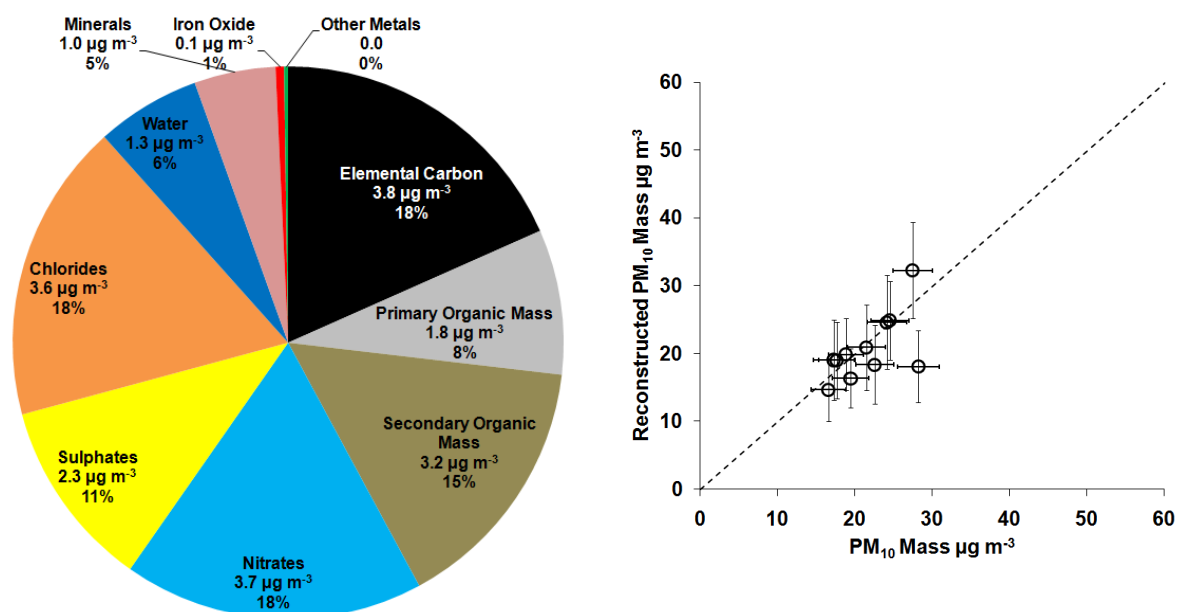
Figure 11: Mean chemical composition of samples in dataset A (left), agreement of reconstructed PM$_{10}$ mass with measured PM$_{10}$ mass (right)

Note: Dashed line is 1:1, uncertainties are expressed at k = 2

These components can be summed to provide a reconstructed mass, this can be used to validate the mass closure model performance; a scatter plot of this comparison is shown in Figure 11 (right). It is clear from this chart that the model performed well. All but one of the reconstructed masses was within the uncertainties expected from the model, of these only 3 days were greater than the uncertainty expected from the PM$_{10}$ measurements alone. The single day which was outside the model uncertainty was 7th November, the Friday following Guys Fawkes Night, when there would have been a large number of bonfires and fireworks displays. This could be considered an unusual chemical composition and it was therefore not wholly surprising that this was not fully captured by the model.

An orthogonal regression analysis of all days resulted in a slope of 1.35 (±0.31) and intercept of -8.42 (±6.88) µg m^{-3}, the correlation coefficient (r^2) was 0.40. When the 7th November was removed, the orthogonal regression analysis resulted in a slope of 1.48 (±0.24) and intercept of -10 (±5.13) µg m^{-3}, the r^2 was 0.77. The correlation coefficient therefore improved markedly when this date is removed. Nevertheless, this comparison is somewhat limited by the low number of measurements available, the low concentrations (mean of dataset A was 21.7 µg m^{-3} compared to 27.7 µg m^{-3} for the whole dataset) and the narrow range (17 – 28 µg m^{-3}).

7.3. Dataset B

The mean chemical composition of the samples in dataset B is shown in Figure 11 (left); the comparison of measured and reconstructed mass is also shown for illustrative purposes (right). Elemental carbon concentrations contributed 18 % to the mass while the organic fraction contributed 20 % to the mass, split 9 % primary and 11 % secondary; this was very similar to dataset A. Chloride salts contributed 16 % and sulphate contributes 9 % of the total mass. Nitrates were the largest contributor to the mass with 25 %; this was 7 % greater than in dataset A. The water associated with these components added a further 5 %; the same as dataset A. The 7 % remaining mass was unidentified; this varied between -6.2 µg m^{-3} and +11.0 µg m^{-3}. This was expected to be made up of the minerals, metal oxides and metals, which were measured directly in dataset A. This assumption was supported by the agreement between the sum of these components found in dataset A (6 %) and the unidentified 7 % in dataset B.
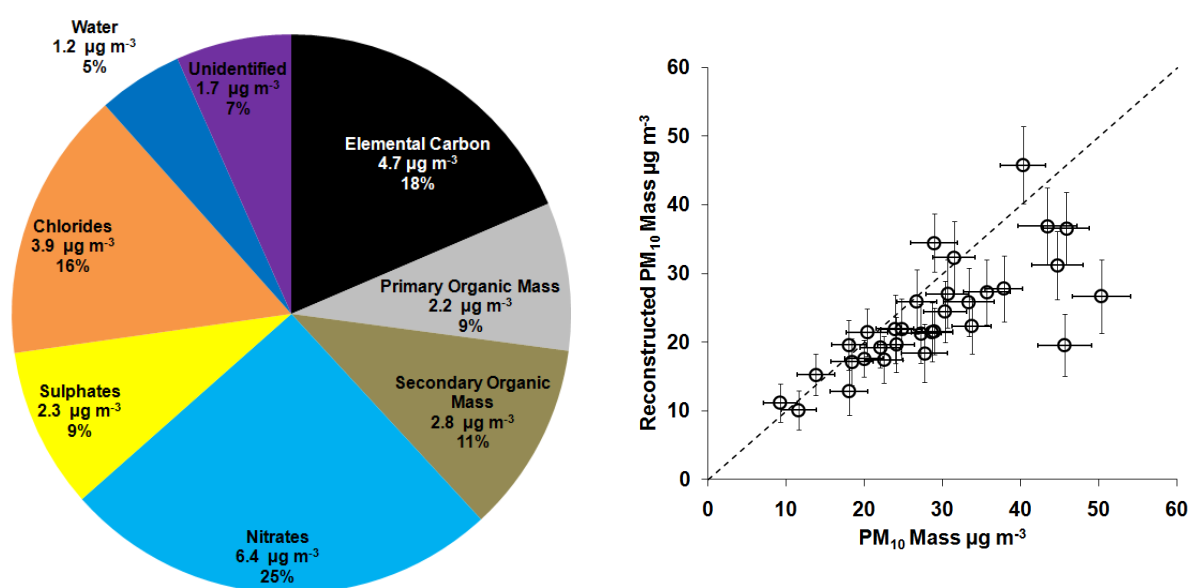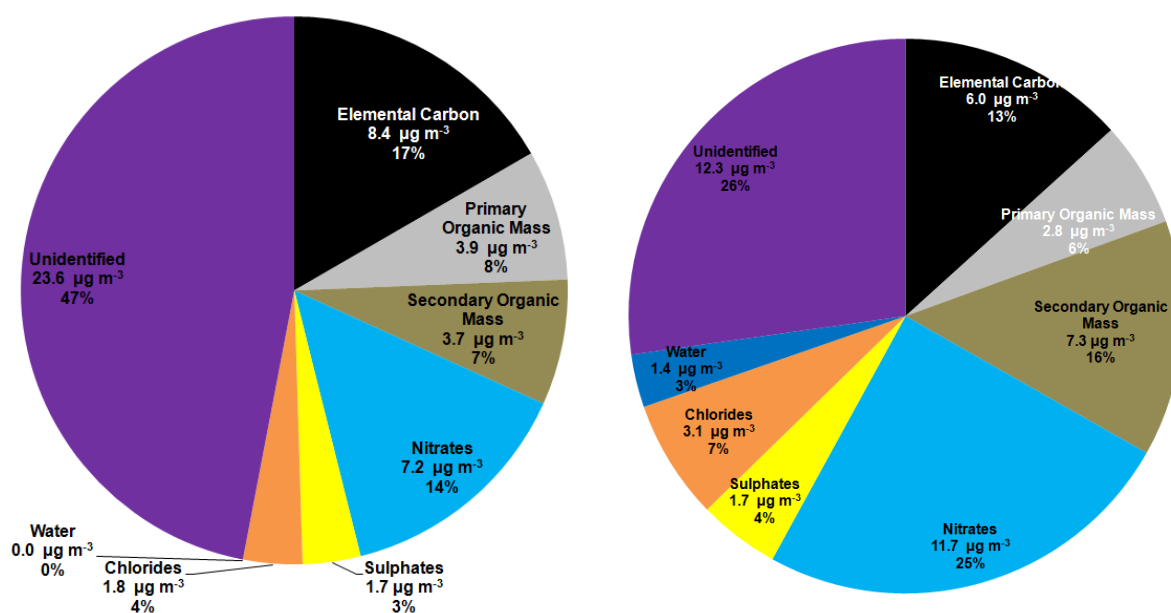

Figure 12: Mean chemical composition of samples in dataset B (left), agreement of reconstructed PM$_{10}$ mass with measured PM$_{10}$ mass (right)

Note: Dashed line is 1:1, uncertainties are expressed at k = 2

7.4. Elevated Concentrations

In recent years Swiss Cottage has breached the EU daily mean limit value of 50 µg m^{-3} but not the annual mean limit value (Fuller and Meston, 2008; Fuller et al., 2009). Understanding the composition of PM during these episodes is clearly very important. Unfortunately only a single day breached the daily mean limit value during this study, this was 5th November, Guy Fawkes Night, when there would have been a large number of bonfires and fireworks displays and is shown in Figure 13 (left). This was a date from dataset B, when no metals concentrations were measured; the unidentified fraction contributed 47 % of the total PM$_{10}$ mass.

Figure 13: Mean chemical composition on 5th November 2008 (left) and on days when PM$_{10}$ concentrations exceeded 40 µg m^{-3} (right)

To assess the chemical composition of days when PM$_{10}$ is elevated, the days when PM$_{10}$ is greater than the 40 µg m^{-3} limit value have been isolated. The metal composition was not measured on any of these days. The mean chemical composition of these days is shown in Table 3 and summarised in Figure 13 (right).

Date	PM$_{10}$ (µg m^{-3})	EC (µg m^{-3})	POAM (µg m^{-3})	SOAM (µg m^{-3})	Nitrate (µg m^{-3})	Sulphate (µg m^{-3})	Chloride (µg m^{-3})	Water (µg m^{-3})	Unidentified (µg m^{-3})	Total (µg m^{-3})
05-Nov	50.3	8.4	3.9	3.7	7.2	1.7	1.8	0.0	23.6	26.7
12-Dec	45.9	7.2	3.3	7.1	10.8	3.1	2.7	2.4	9.3	36.6
06-Nov	45.6	5.9	2.7	1.4	6.2	2.3	1.0	0.0	26.1	19.6
29-Nov	44.7	1.7	0.8	5.8	15.7	0.8	3.6	2.8	13.5	31.2
04-Nov	43.4	6.2	2.9	5.5	15.1	2.3	4.9	0.0	6.5	36.9
07-Dec	40.3	6.6	3.0	13.7	12.0	2.5	4.9	3.1	-5.5	45.8

Table 3: Chemical composition of days when daily mean was greater than 40 µg m^{-3}

The mean chemical composition indicates that the unidentified mass and nitrate are the key components, however, the daily mean chemical composition indicates that the SOAM can contribute substantially.

7.5. Primary and secondary sources

Source apportionment has been used to identify the sources of PM$_{10}$ successfully in London in several studies (Fuller et al., 2002; Fuller and Green, 2004; Fuller and Green, 2006). The same approach has been used to apportion the PM$_{10}$ between primary and secondary sources for the campaign period. The chemical components have then been grouped into primary and secondary source groups as shown in Table 4 compared the predicted split between sources in Figure 14.

Primary chemical component	Secondary chemical component
Elemental carbon	SOAM
POAM	Nitrates
Minerals	Sulphates
Iron oxide	Chlorides
Other metals	Water
Unidentified (dataset B only)	

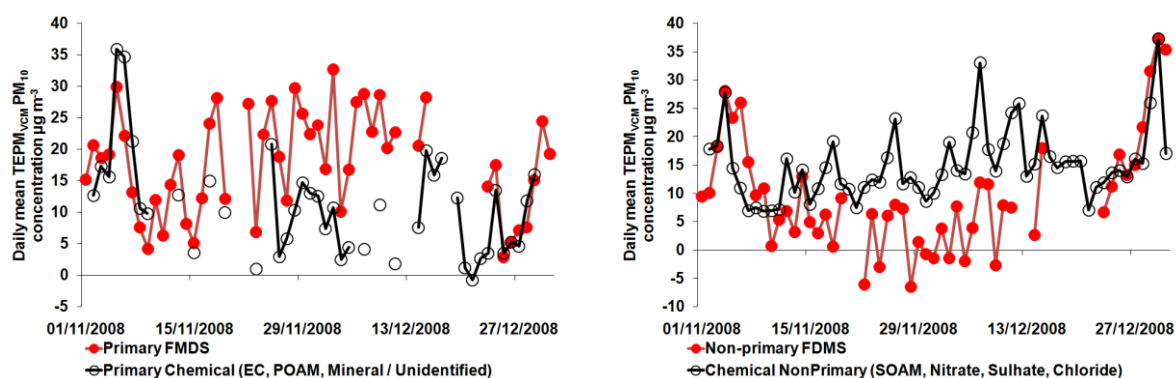**Table 4: Grouping of primary and secondary chemical components**

Figure 14: Comparison been modelled primary and chemical primary PM$_{10}$ concentrations (left) and modelled secondary and chemical secondary PM$_{10}$ concentrations

The general relationship between the source apportionment model and the chemical characterisation are in agreement, especially during the peak periods at the start of November and the end of December. However, the period between mid November and mid December shows a deviation between the source apportionment and chemical assignments of sources which requires further investigation. Nevertheless, this comparison shows a consistency in the two approaches and that the grouping of the chemical components and therefore the sources that we can attribute them to is broadly correct. However, components such as minerals, iron oxide, metals and its surrogate in dataset B (unidentified) is likely to have a number of sources which are both primary and secondary; this may be a source of some of the uncertainty.

7.6.   Mass closure uncertainty

The mass closure uncertainty could be considered large, ± 5.7 µg m^{-3} for data set A and ± 4.2 µg m^{-3} for dataset B, this is approximately 28 % of dataset A and 17 % of dataset B. However, the uncertainty is a combination of many different measurements and assumptions. It is useful to examine what contributes to the uncertainty to improve future applications of the methodology with respect to experimental planning and analysis techniques. The uncertainty in each of the components in datasets A and B are shown in Figure 15.
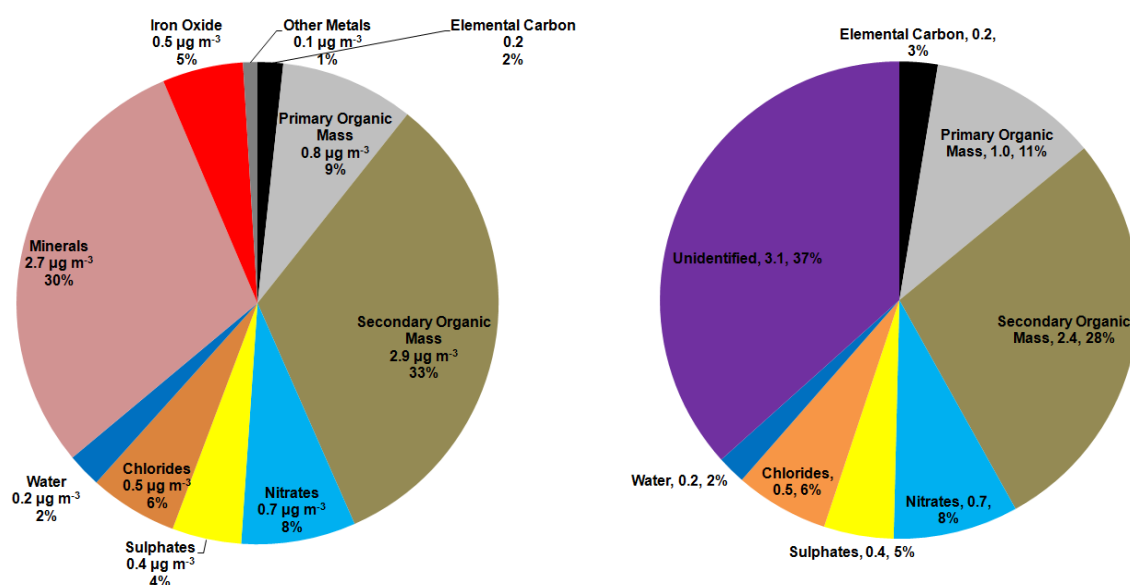

Figure 15: Mass closure uncertainty in dataset A (left) and dataset B (right)

The primary sources of uncertainty in dataset A are the minerals and SOAM. The uncertainty in both these components is driven partly by the measurement uncertainty and partly by the uncertainty in the assumptions regarding the mass associated with the tracer elements. The uncertainty in SOAM is also partly caused by the increased uncertainty due to the application of the regional SOAM as it was not measured directly on these days. Nearly 40 % of the uncertainty in dataset B is caused by the unidentified mass as this is a combination of the uncertainties of all of the components as well as the uncertainty in the PM$_{10}$ measurements.

8. Conclusions

Measuring the chemical composition at Swiss Cottage and undertaking the mass closure analysis has provided a valuable insight into the sources and make-up of PM$_{10}$ at this location. This can inform the understanding of emissions, the targeting of abatement strategies and the assessment of the toxicological components of PM$_{10}$.

This study measured a limited suite of elements to provide a cost effective way of undertaking this analysis with a single sampler. This necessitated, as in all mass closure studies, a number of assumptions regarding chemical composition to establish the mass of the components. Furthermore, the concentration of the components which either regional or distant in source, and therefore uniform in concentration across London, have been taken from measurements made at other sites in London.

This methodology produced of two datasets (A and B) as it was limited to a single sampler and no filter media was suitable for the different analyses. Filters were therefore alternated on a daily basis; this resulted in a chemical composition on one day which included metals and minerals (A) and one which did not (B). There was an excellent agreement between the two datasets, demonstrating that this methodology is a valid way of assessing the chemical composition. Dataset A could be compared directly to the independently measured mass concentration; these two measurements agreed within the calculated uncertainty on all but one day. This was the Friday following Guy Fawkes Night, when fireworks and bonfires would have resulted in an unusual PM chemical composition.

Importantly, throughout the mass closure model, the uncertainties in the measurements have been combined with the uncertainties in the assumptions to provide a realistic assessment of the uncertainty in the reconstructed mass of PM$_{10}$. The model uncertainties were between 16 and 36 %, with a mean of 27 %. These uncertainties could have been reduced by measuring more chemical components, however, this would have necessitated the installation of a second sampler and an expanded range of chemical analysis; this would have substantially increased the cost.

From a local authority point of view, the chemical composition demonstrates that much of mass of PM$_{10}$ comes not from the road but from outside the borough boundary and even outside London. Approximately two thirds of PM$_{10}$ can be considered secondary or natural, being made up of PM formed from gaseous precursors (nitrates, sulphates and SOAM) or sea salt (chlorides). The remaining third is comprised of direct vehicle exhaust (EC and POAM), tyre and brake wear (iron oxide, POAM, metals) and minerals from windblown soil and vehicular resuspension. This attribution of chemical components to sources was demonstrated to agree well with an established source apportionment modelling approach.

The dataset generated is limited as it spans only two months and only included a single breach of the EU daily limit value (Guy Fawkes Night), however, mean concentrations during the campaign agreed well with the seasonal and annual mean. The results are therefore indicative of the composition over the longer term but further analysis of other key periods, such as the summer and long-range transport episodes, or over a whole year would increase the confidence in the results.

9. References

Castro, L. M., Pio, C. A., Harrison, R. M. and Smith, D. J. T., 1999. Carbonaceous aerosol in urban and rural European atmospheres: estimation of secondary organic carbon concentrations. Atmospheric Environment. 33, 2771-2781.

Clarke, A. G., Azadi-Boogar, G. A. and Andrews, G. E., 1999. Particle size and chemical composition of urban aerosols. The Science of the Total Environment. 235, 15-24.

Clegg, S., Brimblecombe, P. and Wexler, A. S., 2009. The Extended Aerosol Inorganics Model Project, University of East Anglia, Retrieved on 14/10/2009 from http://www.aim.env.uea.ac.uk/aim/aim.php.

Defra, 2009. Local Air Quality Management (LAQM) Tools, Department for Environment, Food and Rural Affairs; Scottish Executive; Welsh Assembly Government; and Department of the Environment in Northern Ireland (Defra), Retrieved on 20/01/2009 from http://www.airquality.co.uk/archive/laqm/tools.php?tool=background.

Derwent, R. G. and Malcolm, A. K., 2000. Photochemical generation of secondary particles in the United Kingdom. Philosophical Transactions of the Royal Society.

EMEP, 2002. EMEP manual for sampling and analysis. Co-operative programme for monitoring and evaluation of the long-range transmission of air pollutants in Europe (EMEP), Kjeller, Norway. Report number: EMEP/CCC-Report 8/2007. http://tarantula.nilu.no/projects/ccc/manual/index.html.

EMEP, 2009. EMEP Draft protocol for EC/OC, Retrieved on 15/10/2009 from http://tarantula.nilu.no/projects/ccc/manual/index.html.

EPA, 2003a. Standard operating procedure for PM$_{2.5}$ anion analysis. US Environmental Protection Agency (EPA), Washington. http://www.epa.gov/ttn/amtic/files/ambient/pm25/spec/anionsop.pdf.

EPA, 2003b. Standard operating procedure for PM$_{2.5}$ cation analysis. US Environmental Protection Agency (EPA), Washington. http://www.epa.gov/ttn/amtic/files/ambient/pm25/spec/anionsop.pdf.

EPA, 2004. List of designated reference and equivalence methods. US Environmental Protection Agency (EPA), Washington. www.epa.gov/ttn/amtic/files/ambient/criteria/ref1005.pdf.

Favez, O., Cachier, H., Sciare, J. and Le Moullec, Y., 2007. Characterization and contribution to PM$_{2.5}$ of semi-volatile aerosols in Paris (France). Atmospheric Environment. 41, 7969.

Frank, N. H., 2006. Retained nitrate, hydrated sulfates, and carbonaceous mass in federal reference method fine particulate matter for six eastern U.S. cities. Journal of the Air and Waste Management Association. 56, 500 - 511.

Fuller, G. W., Carslaw, D. C. and Lodge, H. W., 2002. An empirical approach for the prediction of daily mean PM$_{10}$ concentrations. Atmospheric Environment. 36, 1431-1441.

Fuller, G. W. and Green, D., 2004. The impact of local fugitive PM$_{10}$ from building works and road works on the assessment of the European Union limit value. 38, 4993.

Fuller, G. W. and Green, D. C., 2006. Evidence for increasing concentrations of primary PM$_{10}$ in London. Atmospheric Environment. 50, 6134 - 6145.

Fuller, G. W. and Meston, L., 2008. Air quality in London, London air quality network report 13, 2005-6. Environmental Reasearch Group, King's College London, Report number: 13.

Fuller, G. W., Meston, L., Green, D. C., Westmoreland, E. and Kelly, F., 2009. Air quality in London, London air quality network report 14, 2006-7. Environmental Reasearch Group, King's College London, Report number:

Green, D. C., Alexander, J., Fuller, G. W., Quincey, P. and Butterfield, D., 2007. Marylebone Road aethalometer trial report. King's College London,

Green, D. C., Fuller, G. W. and Baker, T., 2009. Development and validation of the volatile correction model for PM$_{10}$ – An empirical method for adjusting TEOM measurements for their loss of volatile particulate matter. Atmospheric Environment. 43, 2132–2141.

Grover, B. D., Eatough, N. L., Woolwine, W. R., Cannon, J. P., Eatough, D. J. and Long, R. W., 2008. Semi-continuous mass closure of the major components of fine particulate matter in Riverside, CA. Atmospheric Environment. 42, 250.

Harrison, D., 2006. UK equivalence programme for monitoring of particulate matter. Report prepared for the Department for Environment, Food and Rural Affairs; Scottish Executive; Welsh Assembly Government; and Department of the Environment in Northern Ireland (Defra), London. Report number: BV/AQ/AD202209/DH/2396. http://www.airquality.co.uk/archive/reports/cat05/0606130952_UKPMEquivalence.pdf.

Harrison, R. M., Jones, A. M. and Lawrence, R. G., 2003. A pragmatic mass closure model for airborne particulate matter at urban background and roadside sites. Atmospheric Environment. 37, 4927-4933.

Harrison, R. M., Jones, A. M. and Lawrence, R. G., 2004. Major component composition of PM$_{10}$ and PM$_{2.5}$ from roadside and urban background sites. Atmospheric Environment. 38, 4531–4538.

Harrison, R. M. and Jones, M. R., 1995. The chemical composition of airborne particles in the UK atmosphere. The Science of the Total Environment. 168, 195-214.

Harrison, R. M. and Yin, J., 2008. Sources and processes affecting the carbonaceous aerosol in central England. Atmospheric Environment. 42, 1413-1423.

Hayman, G., Yardley, R., Quincey, P., Butterfield, D., Green, D., Alexander, J., Johnson, P. and Tremper, A., 2008. Airborne particulate concentrations and numbers in the United Kingdom (phase 2) annual report 2007. National Physical Laboratory (NPL), London. Report number: AS 25. http://www.airquality.co.uk/archive/reports/cat05/0807221457_Particles_Network_Annual_Report_2007_Final_(AS25).pdf.

ISO, 1995. Guide to the expression of uncertainty in measurement. International Organisation for Standardisation (ISO), Geneva , Switzerland.

Japar, S. M., Szkarlat, A. C., Gorse, R. A., Heyerdahl, E. K., Johnson, R. L., Rau, J. A. and Huntzicker, J. J., 1984. Comparison of solvent extraction and thermal-optical carbon analysis methods: application to diesel vehicle exhaust aerosol. Environmental Science and Technology. 18, 231-234.

Jones, A. M. and Harrison, R. M., 2009. The wind speed dependence of the concentrations of airborne particulate matter and NO$_X$. Atmospheric Environment. In press,

Koutrakis, P., Thompson, K., Wolfson, J., Spengler, J., Keleler, G. and Slater, J., 1992. Determination of aerosol strong acidity losses due to interactions of collected particles: Results from laboratory and field Studies. Atmospheric Environment. 26A, 987-995.

Maggs, R., 1999. Particulate pollution in the United Kingdom: Partisol 2025 PM$_{10}$ measurements local site operator procedure manual. Report prepared by Stanger Science and Environment for the Department for Environment, Food and Rural Affairs; Scottish Executive; Welsh Assembly Government; and Department of the Environment in Northern Ireland (Defra), London.

Mückler, P., 1999. Test report on the proof of the equivalence of the concentration measuring instrument Partisol 2000 from Rupprecht & Patashnick Co., Inc. using the reference method in accordance with European standard prEN 12341. RWTÜV Anlagentechnik GmbH, Essen. Report number: 5.0.1/205/90.

Polidori, A., Turpin, B. J., Lim, H.-J., Cabada, J. C., Subramanian, R., Pandis, S. N. and Robinson, A. L., 2006. Local and regional secondary organic aerosol: Insights from a year of semi-continuous carbon measurements at Pittsburgh. Aerosol Science and Technology. 40, 861 - 872.

Robinson, A. L., Donahue, N. M., Shrivastava, M. K., Weitkamp, E. A., Sage, A. M., Grieshop, A. P., Lane, T. E., Pierce, J. R. and Pandis, S. N., 2007. Rethinking organic aerosols: Semivolatile emissions and photochemical aging. Science. 315, 1259-1262.

Schwarz, J., Chi, X., Maenhaut, W., Civis, M., Hovorka, J. and Smolík, J., 2008. Elemental and organic carbon in atmospheric aerosols at downtown and suburban sites in Prague. Atmospheric Research. 90, 287-302.

Seinfeld, J. H. and Pandis, S. N., 1998. Atmospheric chemistry and physics from air pollution to climate change. John Wiley & Sons Inc,

Sillanpää, M., Hillamo, R., Saarikoski, S., Frey, A., Pennanen, A., Makkonen, U., Spolnik, Z., Van Grieken, R., Branis, M., Brunekreef, B., Chalbot, M.-C., Kuhlbusch, T., Sunyer, J., Kerminen, V.-M., Kulmala, M. and Salonen, R. O., 2006. Chemical composition and mass closure of particulate matter at six urban sites in Europe. Atmospheric Environment. 40, 212-223.

Sposito, G., 1989. The chemistry of soils. Oxford University Press, Oxford.

Stribley, T., 2003.Analytical and statistical studies on the provenance and chemistry of PM$_{10}$ in London. Health and Life Sciences, University of London, London. PhD.

Turpin, B. J. and Lim, H.-J., 2001. Species contributions to PM$_{2.5}$ mass concentrations: Revisiting common assumptions for estimating organic mass Aerosol Science and Technology. 35, 602 - 610.

Turpin, B. J., Saxena, P. and Andrews, E., 2000. Measuring and simulating particulate organics in the atmosphere: problems and prospects. Atmospheric Environment. 34, 2983-3013.

Viana, M., Maenhaut, W., Brink, H. M. t., Chi, X., Weijers, E., Querol, X., Alastuey, A., Mikuska, P. and Vecera, Z., 2006. Comparative analysis of organic and elemental carbon concentrations in carbonaceous aerosols in three European cities. Atmospheric Environment. 41, 5972 - 5983.

White, W. H., 2008. Chemical markers for sea salt in IMPROVE aerosol data. Atmospheric Environment. 42, 261-274.

Yardley, R., Quincey, P., Butterfield, D., Green, D., Alexander, J., Johnson, P. and Tremper, A., 2007a. Airborne particulate concentrations and numbers in the United Kingdom (phase 2) - annual report 2006. National Physical Laboratory (NPL), London. Report number: AS 1.

Yardley, R., Quincey, P., Butterfield, D., Williams, M., Green, D., Johnson, P. and Tremper, A., 2006. Airborne particulate concentrations and numbers in the United Kingdom (phase 2) - annual report 2005. National Physical Laboratory (NPL), London. Report number: DQL-AS 028.

Yardley, R., Sweeney, B., Butterfield, D., Quincey, P. and Fuller, G., 2007b. Estimation of measurement uncertainty in network data. National Physical Laboratory (NPL), London. Report number: DQL-AS 037.

Yttri, K. E., Aas, W., Bjerke, A., Cape, J. N., Cavalli, F., Ceburnis, D., Dye, C., Emblico, L., Facchini, M. C., Forster, C., Hanssen, J. E., Hansson, H. C., Jennings, S. G., Maenhaut, W., Putaud, J. P. and Tørseth, K., 2007. Elemental and organic carbon in PM10: a one year measurement campaign within the European Monitoring and Evaluation Programme EMEP. Atmospheric Chemistry and Physics. 7,

Zhou, J., 1997.Chemical characterisation and source apportionment study of PM$_{10}$ in the atmosphere of London. Department of Life Sciences, King's College London, PhD.